An investigation on thin film adhesion measurement methods

CENTRE FOR ANALYSIS AND SYNTHESIS | FACULTY OF ENGINEERING | LUND UNIVERSITY
FILIP SKÖLD AND EVELINA BERGENGREN | MASTER OF SCIENCE THESIS | 2016

An investigation on thin film adhesion measurement methods

- Improving and developing methods to measure adhesive fracture energy between thin polymer film and aluminium foil in packaging material

Evelina Bergengren & Filip Sköld

Supervisor at Tetra Pak: Nils Toft

Supervisor at LTH: Baozhong Zhang

Examiner: Reine Wallenberg

Acknowledgements

We would like to thank the following persons for their contributions during our thesis work.

Nils Toft
For great discussions about truth, life and the future. For all the help during our thesis and for being such an inspiring and cool person.

Anna Andersson, Annika Andersson, Eskil Andreasson, Jakob Elamzon and Kristina Svensson
For discussions and good inputs during our work.

Anna Ekström and Elin Postlind
For all discussions in dark times and desperate moments.

Martin Gunnarsson, Anders Andersson and Isabella Eriksson
For helping us with the tensile tests.

Bret Hamburger, Jonas Galea, Michelle Lindström and Ilona Lindbergen
For great patience and help with the measuring equipment and purchases.

Baozhong Zhang
For being our supervisor at LTH.

• • • • • • • • • • • • • • • •

During this thesis all work has been performed both by Evelina and Filip, but with own areas of responsibility. Filip has been responsible for regular peel tests and Evelina has been responsible for peel arm reinforcement and the DuckFace.

What keeps your packages together?

By: Evelina Bergengren & Filip Sköld

Based on the Master Thesis: *An investigation on thin film adhesion measurement methods*

Have you ever taken a closer look at the packages in your home? They consist of several layers of different materials, among them layers of polymer. They all contribute to protect the product. For a packaging company it is very important to ensure that the layers in the package are held tightly together, in order to withstand the stresses associated with transportation, storage and consumer use.

So what is it that makes these layers stick together? The phenomenon is called *adhesion* and describes how strong two surfaces are joined. Measuring adhesion is a tricky task. It is difficult to measure without affecting the result. Imagine that you are measuring the temperature of your steaming hot coffee with an ice cold thermometer. The coffee will then be cooled by the thermometer and by that, the measured temperature will be affected. Though, it is possible to come close to measuring adhesion by separating two surfaces. The measured value is called *adhesive fracture energy*.

Adhesive fracture energy is often measured by performing peel tests. A peel test is done by letting a machine measure the force needed to pull off one polymer layer. One of the most common ways to peel off the layer is in 90° in relation to the rest of the material. This can be seen in the picture below. The layer that detaches is called peel arm. If the peel arm is very thin it will deform, which requires energy. The measured force from the peel test will therefore contain both the adhesive fracture energy and the deformation of the peel arm.

Packaging material during a 90° test

To extract the adhesive fracture energy from the force, a method called ICPeel can be used. The method calculates how much energy was lost to deform the peel arm. It proved to be difficult to calculate the energy lost in the bend that arises when peeling in an angle.

Another way to separate the layers, without bending the peel arm, was developed. In this method the peel arm is pulled along the sample with a peel angle of 0°. The difference between peeling in 90° and 0° can be seen in the following pictures.

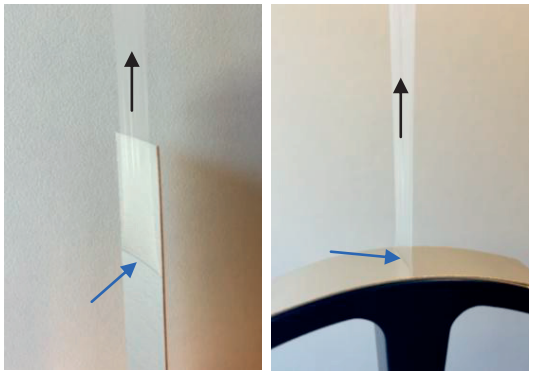

To the left a 0° test, to the right a 90° test. Peeled in direction marked by black arrow. The blue arrow marks the crack.

Along with that the layer detaches, a crack is formed between the peel arm and the rest of the material. The crack propagates along the material. The *crack propagation speed* depends on how fast the machine is pulling the peel arm.

The adhesive fracture energy was measured, calculated and plotted using a number of different crack propagation speeds.

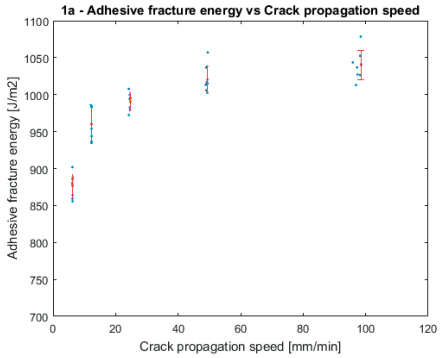

Adhesive fracture energy vs. crack propagation speed

As seen in the figure above, the adhesive fracture energy increases when the crack propagation speed is increased. Adhesion is very complex and arises from a number of different mechanisms. A possible explanation for why the adhesive fracture energy increases with increasing speed could be that some of these mechanisms behave differently at high and low speeds.

This can be compared to ripping off a band aid; you can either do it fast and very painful or slowly and less painful. How fast you do it will affect the result. Thus there is not an absolute value of adhesive fracture energy, but it changes by the way you are measuring it.

Abstract

In this thesis methods for measuring and calculating the adhesion between the inside polymer layer and the aluminium layer of Tetra Pak's packaging materials have been investigated. This was done both by exploring the possibilities of combining peel tests with the ICPeel method, and by developing ideas for new measuring methods. One of the ideas was built on a test setup for a close-to normal direction test, where the materials were separated in the normal direction in a controlled manner. Another idea involved separating the layers by pulling the inside layer at an angle of 0° in relation to the aluminium layer, whereafter the adhesive fracture energy was extracted using a formulated equation. The thickness profile of the inside layer and its influence on the results was also briefly investigated.

The ICPeel method was found to have limitations when using as thin films as in this thesis, since the samples were subjected to strains larger than what ICPeel theory can account for. Attempts to reduce the strain were made by reinforcing the peel arm using tape. However, the tape proved to have too poor adhesion to the peel arm in order for these tests to be conducted. The close-to normal direction test was also problematic due to the insufficient adhesion of the tape. The most promising method proved to be the 0° test, which generated results suggesting how the adhesive fracture energy depends on test rate.

Table of contents

1 Introduction 1
2 Background 2
2.1 Tetra Pak 2
2.2 Packaging material 2
2.3 Polyethylene 3
2.4 Extrusion coating and lamination 5
2.5 Adhesion 6
2.6 Tensile test 7
2.7 Peel test 9
2.8 ICPeel theory 10
2.9 SEM 11
2.10 Board delamination 11
2.11 FTIR 11
2.12 Tape 11
3 Material preparation 12
3.1 Materials 12
3.2 Tensile test 13
4 Study 1 14
4.1 Method 14
4.2 Result 19
4.3 Discussion 25
5 Study 2 26
5.1 Ideas for alternative test setups 26
5.2 Method 30
5.3 Result 35
5.4 Discussion 41
6 Adhesion discussion 42
7 Conclusion 42
7.1 Proposals for future work 43
8 Bibliography 44
9 Appendix 47

1 Introduction

This thesis was written in collaboration with Tetra Pak, which is a global packaging company. Tetra Pak's packaging material consists of an outside polymer layer, paperboard and an inside polymer layer. An aluminium foil is added between the board and the inside layer when the barrier properties need to be improved. The adhesion between the inside layer and the aluminium layer is of great importance; if the adhesion is too poor the barrier properties may be affected. At Tetra Pak adhesion is currently being estimated with the force needed to peel off the inside layer from the aluminium layer. During the test, energy losses in the peel arm occur, resulting in a peel force containing both adhesion and deformation of the peel arm. Instead it would be preferred to obtain a value for the adhesion alone. This would give a better understanding of how the adhesion is affected in different process steps and how the adhesion between the packaging material layers is affecting the properties of the finished package. An additional benefit of being able to measure adhesion is that it would enable the adhesion in different kinds of packaging materials to be compared to each other.

Initially in the thesis work the expression "true adhesion" was introduced, but exactly what the term 'true' was referring to was not completely defined. There were different views of if adhesion could be described by an absolute value or if it depends on external factors. Tetra Pak has tried to obtain an adhesion value by using ICPeel methodology with peel tests. The results from the tests have been indicating that the theory might be insufficient when having very thin peel arms.

During the thesis two main studies have been carried out, the first aiming to understand if and how ICPeel theory can be used to extract a value for adhesion from peel tests made on thin film laminates. In this study regular peel tests in both 90° and 180° have been performed. The resulting peel force from the measurements has been processed with ICPeel methodology to calculate an adhesion value for the interface. The second study consisted of other approaches for measuring adhesion. This study could be divided into two parts; one where peel tests with modifications were conducted to isolate phenomena to explain why the ICPeel method could be suboptimal, the other investigating ideas for new measuring methods to obtain a value for adhesion. One idea was aiming to perform a close-to normal direction test. Another idea was to detach the inside layer by pulling it in 0° in relation to the sample surface.

The scope for the thesis was formulated in the following questions:

- Can ICPeel be used to extract a value for adhesion from regular peel tests?
- Is it possible to develop an approach that enables the combination of peel tests and the ICPeel method?
- Are there any other potential approaches to measure adhesion?
- Does true adhesion exist?

2 Background

Tetra Pak needs to measure adhesion in order to be able to compare different packaging materials and to verify that a material is meeting its specification requirements. It is also of great interest to understand the mechanism of adhesion to be able to design the packaging material in a way that optimises the package. It is also desirable to ascertain how adhesion between packaging material layers is affected in the manufacturing process.

Adhesion is a measure of how strong two surfaces stick together. Today the method used to estimate adhesion at Tetra Pak is peel testing, which is done by measuring the force needed to pull off one layer from the rest of the packaging material. The force required to separate the layers is called peel force. To quantify the adhesive fracture energy from the peel force, several contributions in form of energy losses in the peel arm need to be taken into account. The peel force from different packaging materials can therefore not be compared, due to differences in the peel arm properties. Tetra Pak has been working on approaches for obtaining the adhesive fracture energy from peel tests as well as testing new methods for measuring it. To calculate the adhesive fracture energy from peel tests the ICPeel method (from Imperial College, U.K.) has been used. However, problems have been encountered when having very thin inside layers (around 20µm) i.e. very thin peel arms. Attempts to obtain adhesion without having to consider energy losses in a peel arm have been made in experiments where material layers were pulled apart in the direction normal to the interface. It proved to be very difficult to obtain a clear split between the layers.

2.1 Tetra Pak

Tetra Pak is a global packaging company that offers their customers packaging solutions throughout the whole process chain. Their vision is to make food safe and available everywhere, and their packages are available in more than 170 countries around the world. In 2015 Tetra Pak had 23600 employees and a net sale of €11,9 billion. [1] The brand promise “Protects what´s good” is referring to protect not only food but people, the future and the environment as well. [2]

Material Design is a key competence area within Tetra Pak. One of the aims for Material Design is to reach a deeper understanding of the packaging material behaviour mainly by exploring three areas: adhesion, barrier and fracture mechanics. A generally important aspect of the packaging material behaviour is to be able to confirm that the layers are optimally adhered to each other in order to withstand the stress associated with transportation, storage and consumer use without detaching from each other. Due to the potential risk of influencing the oxygen barrier it is especially important that the adhesion between the layers closest to the product is strong enough. If the layers are partially detached from each other oxygen diffusion is increased, influencing the nutritional value of the product. Due to economical and environmental aspects it is also desirable to use as thin layers as possible. A better understanding of adhesion and a method to measure it would enable the company to optimise and develop new and improved packaging materials.

2.2 Packaging material

The packaging material at Tetra Pak is designed of paperboard, polymer layers and when an aseptic package is needed, an aluminium layer (see **Figure 2.1**).

The core of the packaging material is the paperboard, which gives stability to the final package. On the outside of the paperboard is a polyethylene layer, protecting the board from outside moisture. On the inside of the paperboard is an aluminium foil layer, adhered with polyethylene. The aluminium layer functions as a barrier for light and oxygen which could otherwise degrade the product in the package. Closest to the product is an inside polymer layer adhered to the aluminium foil, functioning as sealing layer. [3] [4]

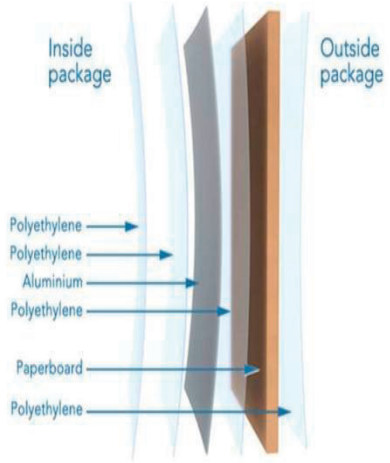

Figure 2.1 Schematic figure of packaging material [4]

2.2.1 Paperboard

The paperboard used in the packaging material is called liquid packaging board and typically consists of five layers (see **Figure 2.2**). The outermost layer is a clay coat consisting mostly of calcium carbonate, which gives it a smooth and white surface good for printing. The layer beneath the clay coat consists of bleached fibres, which also contributes to the whiteness and smooth surface. The next two layers in the board are unbleached fibres and pulp, which give the board stiffness and strength. The last layer of unbleached fibres provides the board with tensile strength. [5]

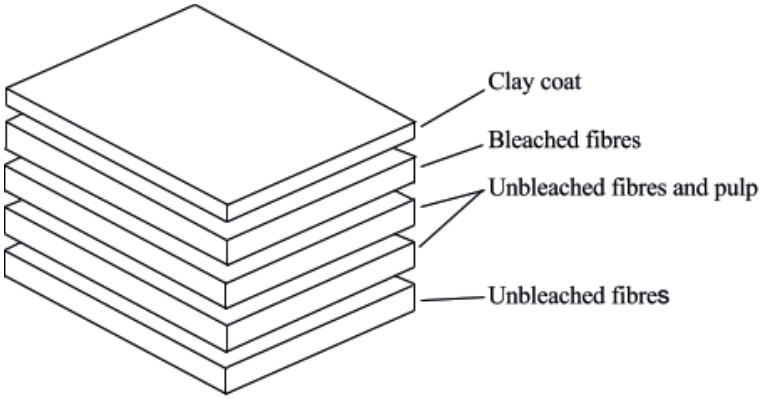

Figure 2.2 Structure of paperboard

2.3 Polyethylene

Polyethylene (PE) is the most common polymer in the world and is mainly used in packaging industries [6]. PE is one of the simplest polymers using ethylene as monomer. The structure of ethylene is shown in **Figure 2.3**. Though the monomer is simple there are several ways to polymerise PE to give it diverse mechanical properties. Typical PE is ductile with high impact strength but lesser

hardness, rigidity and strength. These properties can be tweaked by changing the amount of branching resulting in a density change. The different grades of PE are divided into groups where the most commonly used are Low Density PE (LDPE), High Density PE (HDPE) and Linear LDPE (LLDPE). PE is semi crystalline which means that it has both crystalline and amorphous regions [7]. A description of the grades of PE used in this thesis follows.

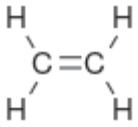

Figure 2.3 Ethylene, the monomer in polyethylene

2.3.1 LDPE

LDPE is by definition PE with a density of 0.92-0.94 g/cm^2 [8]. LDPE is polymerised using free radical polymerisation which gives it a large amount of branching, around 20-33 branch points per 1000 carbon atoms, with long branches [9] (see **Figure 2.4**). The large amount of branching gives LDPE a lower crystallinity and hence a lower density compared to HDPE [10]. The polymerisation process of LDPE also gives a broad molecular weight distribution. The properties of LDPE are very well suited for packaging material films. [7]

2.3.2 LLDPE

LLDPE is as the name suggests a more linear version of LDPE, which is made by copolymerisation of ethylene and α-olefins [11]. This polymer has a narrower molecular weight distribution and shorter side chains than LDPE (see **Figure 2.4**). This makes it more crystalline and therefore having a higher tensile strength and higher impact resistance. LLDPE is an intermediate between HDPE and LDPE regarding density and properties [12]. LLDPE has begun to compete with blends of HDPE and LDPE in film blowing and casting due to these intermediate properties. [7]

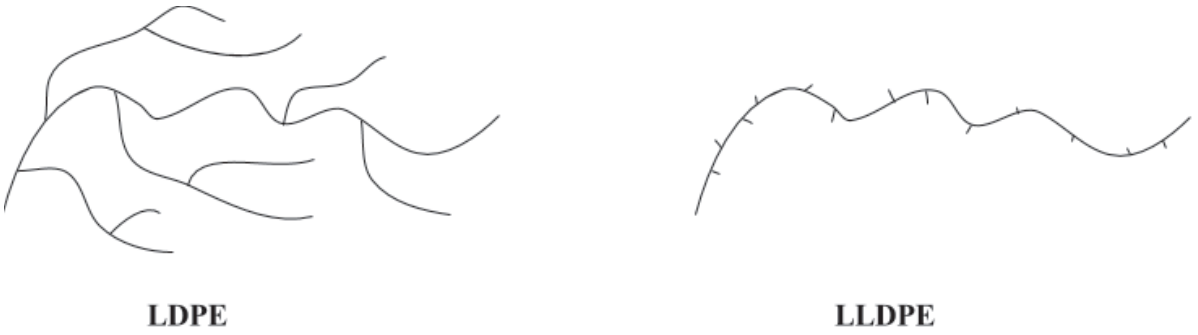

Figure 2.4 Schematic figure of LDPE and LLDPE

2.3.3 mPE

mPE is a blend of LDPE and metallocene catalysed LLDPE. [3] Metallocene catalysts are organometallic compounds which can be used to produce polymers with entirely new properties. [13] During the polymerisation of LLDPE the metallocene catalyst is used to control the molecular weight distribution of the polymer. [7] By changing the catalyst different grades of LLDPEs can be produced. The blend of LDPE and LLDPE is rationed in a manner that produces a polymer blend with properties suited for extrusion lamination. The polymer layer should not contract, but create a homogenous layer with even thickness. [3]

2.4 Extrusion coating and lamination

In the packaging material manufacturing process a laminator is used. A typical laminator has three lamination stations. In every station there is at least one extruder which melts a polymer by applying heat and shear forces. The polymer is extruded to a die and drawn down into a nip. The nip consists of two rolls, a chill roll which cools the melted polymer, and a pressure roll which applies the nip pressure. In the first station the board and the aluminium layer are joined together by a lamination layer of LDPE. The second station applies the inside layer to the aluminium layer by coextruding an adhesive polymer and mPE. In the third station the board is coated with an outside layer of polyethylene. The process for the first two stations is shown in **Figure 2.5**. The thickness of the polymer layers is controlled by the extruder output and the line speed. The final properties of the lamination layers and the adhesion between them are influenced by the molecular architecture in the polymers, as well as the cooling rate and degree of orientation which in turn is controlled by process parameters such as temperature of the polymer melt and the chill roll. [14]

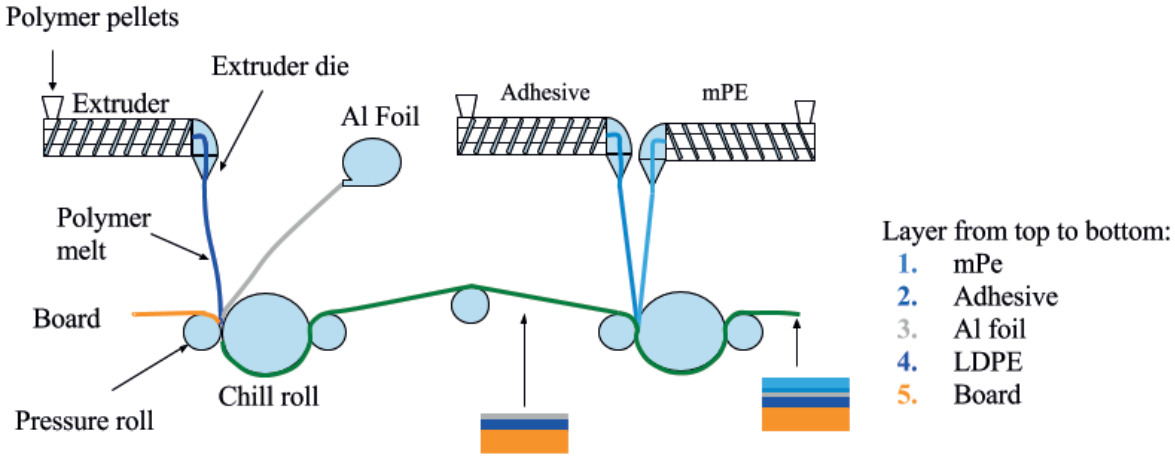

Figure 2.5 Schematic figure of the extrusion coating and lamination process

The outcome from the laminator is packaging material consisting of several layers. The directions in the packaging material are referred to as machine direction (MD) which is the direction it was pulled in the laminator, and cross direction (CD) which is the direction perpendicular to the machine direction (see **Figure 2.6**). The different layers are not completely homogenous and can have variations in thickness in both directions. The material has different properties in different directions, due to orientation of the polymer influenced by pulling in the machine direction in the laminator, and due to the orientation of the fibres in the board. [3]

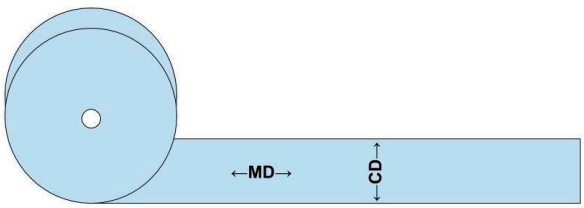

Figure 2.6 Definition of Machine Direction (MD) and Cross Direction (CD) of packaging material

2.5 Adhesion

The phenomenon of two surfaces sticking together is called adhesion. [15] It is a complex concept with contributions from various mechanisms. [16] There are several theories of which mechanisms are contributing to the adhesion. The strength of an adhesive joint often arises due to a mixture of the different mechanisms. Which ones involved depends on the nature of the substrates and the adhesive forming the joint. [17] Furthermore, the adhesion can be thought of broken down into three directional fractions; adhesion in x-, y- and z direction. [18] This is defined in **Figure 2.7**. Depending on the method used and the load case it generates, different amounts of the directional fractions are measured. For a more complete understanding of the adhesion, all three directional components would preferably be measured separately. [18] In adhesion measurements the term *adhesive fracture energy* is used, which refers to the energy needed to separate two surfaces from each other. The adhesive fracture energy is both temperature and test rate dependent. [19]

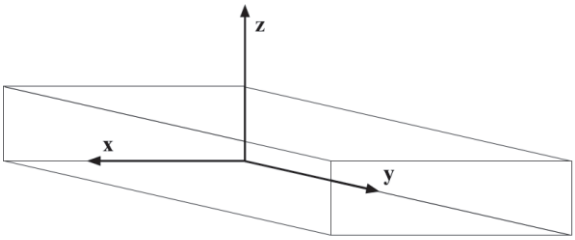

Figure 2.7 Definition of the three different directional adhesion fractions x, y and z

2.5.1 Adhesion theories

There are several theories describing which mechanisms are causing adhesion. The mechanisms are not contradictory but coexists. It is important to understand which mechanisms are present at an interface to predict how the adhesion is affected by environment changes.

The physical adsorption theory describes adhesion as the dipole attraction forces between two surfaces at an interface. [16] The theory includes contributions from both permanent and induced dipoles known as Van der Waal's forces. *The chemical bonding theory* describes adhesion as the chemical bonds between the adherents. These chemical bonds involve hydrogen, covalent and ionic bonds. [15] The binding type and bond strength can be predicted in advance, hence a suitable adhesive can be used to obtain the preferred adhesion between the surfaces. [16] *The diffusion theory* addresses the inter diffusion at the interface of two polymers and can be described as the polymer chains diffusing into the other polymer matrix and becoming entangled. [20] In order for this theory to be applicable the polymers must be compatible and the temperature must be held over the glass-transition temperature (Tg), i.e. have mobility. [21] *Mechanical interlocking* occurs when a surface is uneven and has cavities or pores. [20] When they get filled with a polymer that hardens, the surface and the polymer will be adhered by mechanical interlocking. [15] Clean surfaces adhere well while dust, grease and other contaminants on the surface will weaken the adhesion. When applying an adhesive, contaminants will weaken the adhesion in parts of the interface. Some adhesives can dissolve the contaminants while most will get weaker adhesion. [20] [21]

2.5.2 Modes of failure

When separating two surfaces from each other, the failure can occur at different sites in the material. This is illustrated in **Figure 2.8** below. If the failure arises in either of the adherends, the failure mode is called *cohesive failure in adherend*. A failure in the adhesive is called *cohesive failure in adhesive*. If the failure occurs between the adherend and the adhesive, the term *adhesive failure* is used. This is the desired failure mode in this thesis, since the aim is to measure the adhesion in the interface of the aluminium layer and the inside layer of the material. It is also possible to obtain a mixture of failure modes. [17]

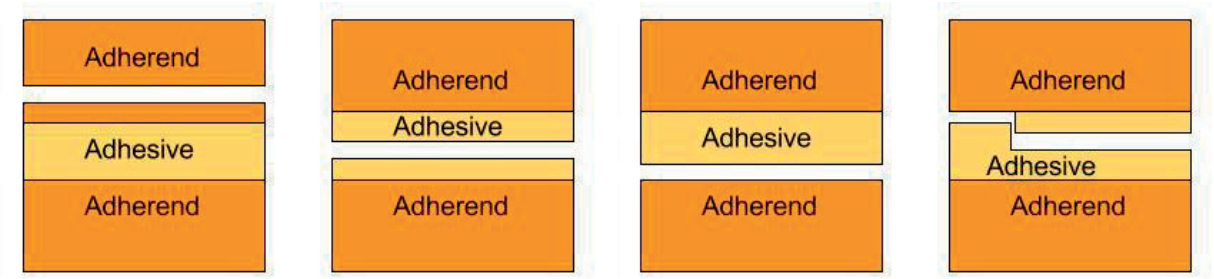

Figure 2.8 Modes of failure from left to right; cohesive failure in adherend, cohesive failure in adhesive, adhesive failure, mixture of failure

2.6 Tensile test

During the thesis an Instron 5565 tensile tester was used to measure the tensile properties of the materials. A picture of the machine can be seen in **Figure 2.9**. The input parameters include the speed (crosshead speed) and distance (extension) the upper clamp moves. The output is usually time, load and extension. When performing tensile tests an extensometer can be used together with the tensile tester to obtain a more exact tracking of the displacement. [22] Tensile tests are usually performed on dog bone shaped specimens in order to ensure that the deformations in the material during the test are

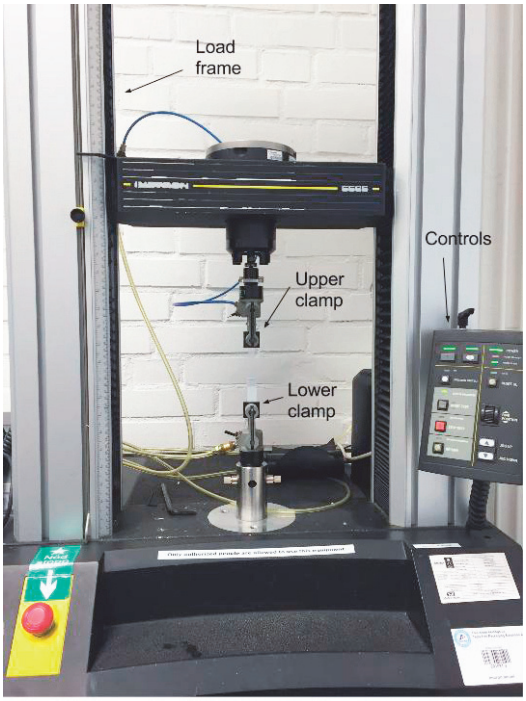

Figure 2.9 Picture of a tensile tester with clamps, load frame and controls marked

confined to the narrow region and thereby reduce the risk of sample rupture occurring at the ends of the specimen. [23] The thickness is measure with a digimatic indicator which uses a stem that is pushed down towards the material and thereby measuring the thickness.

In a tensile test the relationship between stress and strain is analysed using a tensile tester. The stress is measured in Pascal (N/m^2). Strain is a measurement of the elongation of a material. There are two kinds of stress and strain; engineering and true. [24] The most commonly used is the engineering stress-strain where the stress is described as the force divided by the original cross section area. The engineering strain is described as the ratio between elongation and original length. The true stress accounts for the shrinking of the cross sectional area of the material during tensile deformation and the true strain is the natural logarithm of the ratio between the actual length and the original length. [25] The expressions for the different stresses and strains are:

Engineering stress: $\sigma_e = \frac{P}{A}$

Engineering strain: $\varepsilon_e = \frac{l - l_0}{l_0}$

True stress: $\sigma_t = \sigma_e * e^{\varepsilon_t} = \sigma_e(1 + \varepsilon_e)$

True strain: $\varepsilon_t = \ln(\frac{l}{l_0}) = \ln(1 + \varepsilon_e)$

Where P is the force, A is the cross section area, l is the length at the end of the test, l_0 is the original length, σ_e is the engineering stress, ε_e is the engineering strain, σ_t is the true stress and ε_t is the true strain.

A typical stress-strain curve for low strains is bilinear, thus having two distinct regions; an elastic region and a plastic region which is separated by the yield point (see **Figure 2.10**).

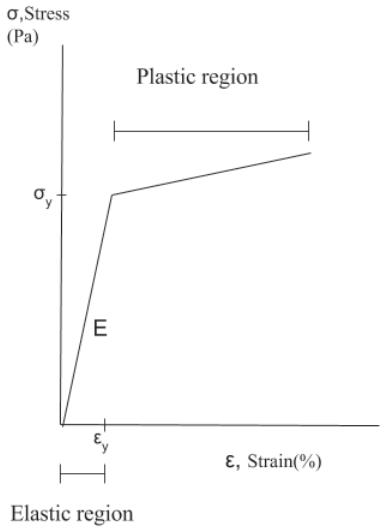

Figure 2.10 Typical stress-strain curve for low strains where ε_y is the yield strain, σ_y is the yield stress and E is young's modulus

A typical stress-strain curve for PE has two yield points (σ_{y1} and σ_{y2}), where the first yield point can be traced to fine slip of lamellae while at the second yield point coarse slip is present. [26] This is visualised in **Figure 2.11**. Fine chain slip refers to tilting of chains and small deformations within the lamellae while coarse chain slip refers to when blocks of lamellae are sliding against each other. [27]

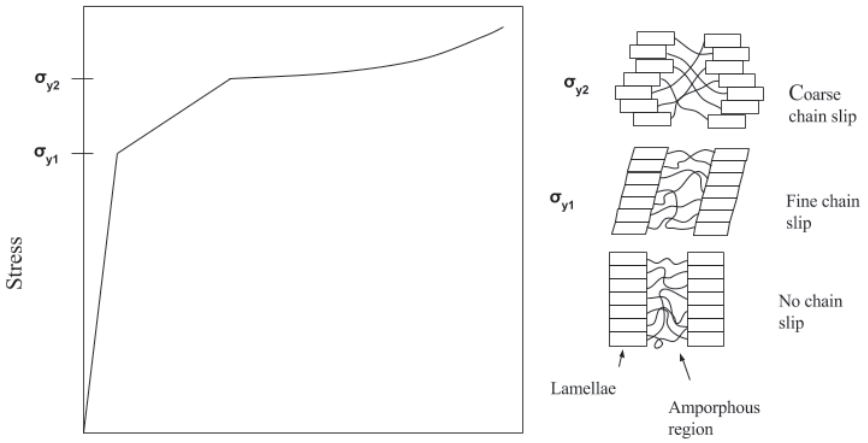

Figure 2.11 Typical stress-strain curve for PE, notice that the curve has two yield points. To the right the mechanisms for the different yield points are shown

2.6.1 Elastic behaviour

When a polymer is subjected to stress in a tensile manner it first behaves elastically, meaning that if the stress is relieved the polymer will return to its starting configuration. [28] All energy used to elongate the polymer is stored inside it and will be released instantly when the stress is removed. The strength of a material can be described by the E-modulus which is the slope of the linear-elastic region in the stress-strain diagram; the E-modulus originates from Hooke's law which explains the linear relationship between stress and strain. [29]

2.6.2 Plastic behaviour

When the stress reaches the yield point (σ_y) of the material it will start to deform plastically instead of elastically. After the yield point the material will continue to deform plastically until it breaks, this is called the plastic region. The deformation is irreversible; the energy used to deform it is lost in the process instead of stored in the material. [7]

2.7 Peel test

Peel testing is a commonly used method for measuring adhesion between thin layers. A peel test is conducted in a tensile tester, where a sample is peeled apart while the force needed to do this is measured. In a peel test the peel angle is usually either 90^o or 180^o (see **Figure 2.12** a) and b)). An 180^o peel test is performed by mounting the sample in the clamps and pulling it apart. When peeling in 90^o a "German wheel" is used in order to maintain a constant peel angle of 90^o. The wheel is mounted in the tensile tester instead of the lower clamp, where it can spin with insignificant friction. [30] The sample is adhered to the wheel with double-sided tape and the peel arm is fixated in the upper clamp.

The force needed to peel the layers apart depends on temperature, peel rate and geometry of the peel arm. These parameters need to be taken into account in order to obtain comparable values of adhesion. [31] The adhesive fracture energy from a peel test is a mixture of adhesion in x-, y- and z-direction. [32]

a ***b***

Figure 2.12 Test setup for peel tests in **a)** 90° **b)** 180°

2.8 ICPeel theory

ICPeel is a method used for calculating the adhesive fracture energy (G_a) from a peel test with a specific peel angle (θ). This method requires the tested material to be adhered to a rigid substrate. [32] To analyse the adhesive fracture energy, three different energy terms must be considered; the stored energy in the peel arm (elastic deformation), the energy dissipated during tensile deformation in the peel arm (plastic deformation) and the energy dissipated due to bending of the peel arm. The bending arise due to that root rotation occurs locally ahead of the peel front creating a local angle, θ_0. There are two extreme cases, i) $\theta_0=0$ where no root rotation occurs and ii) $\theta_0=\theta$ when the peel arm have zero bending modulus. A more likely situation is when $0<\theta_0<\theta$ and the energy is portioned between the bending area and the rest of the peel arm. If these three energy terms are taken into account in the calculations this method is considered to be 'geometric-independent', and the same adhesion value should be obtained regardless of peel angle.

According to ICPeel theory the energy contributions in a peel test can be described by:

$$G_a = \frac{1}{b}\left[\frac{dU_{ext}}{da} - \frac{dU_s}{da} - \frac{dU_{dt}}{da} - \frac{dU_{db}}{da}\right] \quad (1)$$

Where G_a is the adhesive fracture energy per area unit, b is the width of the sample, da is the crack length, U_{ext} is external work, U_s is the energy stored in the peel arm, U_{dt} is the energy dissipated during tensile formation of the peel arm and U_{db} is the energy dissipated during the bending of the peel arm close to the peel front. The theory requires a stress-strain curve to be fitted either by a bilinear fit or by a power law fit. The bilinear fit is described by the E-modulus until the yield point, whereafter it is expressed as a linear function of the E-modulus. The power law fit is expressed by: [32]

$$\sigma = \left(\frac{\varepsilon}{\varepsilon_y}\right)^n \quad (2)$$

Where σ is stress, ε is strain and ε_y is the yield strain. For more in depth theory about ICPeel, the authors recommend the article "Peeling of flexible laminates" by A. Kinloch [32].

2.9 SEM

A Scanning Electron Microscope (SEM) is used to obtain information about topography and/or composition of a sample. Images from SEM have much higher resolution than pictures from a light microscope since the technique is not limited by the wavelength of visible light but by the wavelength of electrons. A SEM is focusing an electron beam on a solid sample. [33] The electrons interact with the atoms at the surface of the sample and scatter. The scattered electrons have different energies depending on the scattering mechanism. Detectors inside the SEM capture the electrons and give information about either topography or composition, depending on which electrons are detected. Samples that are non conducting need to be coated with a conducting material to avoid charging effects. [34]

2.10 Board delamination

To obtain strength in the x and y-direction of the board, the fibres are oriented lengthways in the material during the manufacturing process. This results in an anisotropic material which is less resistant to tensile stresses in the z-direction. [35] The maximum load that the board can withstand before delaminating is referred to as the z-direction strength. [36]

Because of the more strenuous load in a 90° peel test compared to a 180° peel test there is reason to suspect that the risk for board delamination is greater in a 90° test than in 180° test. If so, the energy losses due to this phenomenon would have to be taken into account while doing peel tests.

2.11 FTIR

FTIR is an abbreviation for Fourier Transform InfraRed spectroscopy and is a method for identifying composition and quantity of substances in a sample. The technology utilizes the phenomenon that every individual kind of molecule has a unique ability to absorb light with different wavelengths. [37] The sample is irradiated with infrared radiation, which is partly absorbed and partly transmitted through the sample. A detector collects the transmitted light and forms a spectrum which represents the molecular fingerprint of the material. To obtain an identification of the substances present in the sample, the signal is converted into a frequency spectrum by letting a computer decode the signal by using Fourier transformation. The spectrum from the FTIR shows the absorption peaks of the material where the peak amplitude is a direct indication of the quantitative amount of the substances. [38]

2.12 Tape

In this thesis several tapes were tested. The function of the tapes was to adhere the inside layer or the aluminium layer to different surfaces in the test setups. When using adhesives on thin polymer layers it is important that substances from the adhesive does not migrate through the layer and affect the adhesion on the opposite side i.e. the interface between the aluminium layer and the inside layer. FTIR was used to investigate whether low molecular substances from the tapes migrated through the inside layer. A previous master thesis investigated whether it was possible to find glue that has high enough adhesion, but does not migrate. [39] Unfortunately, this was not possible with the glues selected.

3 Material preparation

The work in this thesis was divided into two different studies. Study 1 contained standard 90°- and 180° peel tests which were analysed with ICPeel theory. This study was done to improve and troubleshoot the method used in previous studies at Tetra Pak. Study 2 contained testing and analysing the ideas from the authors. This study aimed to create new methods to measure adhesive fracture energy. Properties of the materials used have been analysed as well.

The part describing material preparation is common for both studies, while the methods, results and discussion were divided and described for each of the two studies.

3.1 Materials

Two different packaging materials were used, with different thickness of the inside layer. The inside layer consisted of two materials; mPE and Ethylene Acrylic Acid (EAA) which is an adhesive suitable for aluminium and mPE [40] . Three variations of each material were produced; one full packaging material, one with inside- and aluminium layer and one with only the inside layer. The thicknesses are specified in gram per square meter (gsm). The materials are shown in Table 1.

Table 1 Description of the six variations of material

Name	Gsm (EAA + mPE)	Consists of
1a	6 + 42	Full packaging material
1b	6 + 42	Inside- and aluminium layer
1c	6 + 42	Inside layer
2a	6 + 19	Full packaging material
2b	6 + 19	Inside- and aluminium layer
2c	6 + 19	Inside layer

Material 1a/2a were used to do regular peel tests and 0° tests, material 1b/2b were used to reinforce the aluminium layer and to do tests in z-direction, and material 1c/2c were used to obtain the tensile properties of the inside layer.

3.1.1 Extrusion coating

When the different variations of the materials were produced, different settings were used in the laminator. Full packaging material was produced by operating the laminator according to standard procedure. Material b (inside- and aluminium layer) was produced by turning off the first extruder (see **Figure 2.5**), which resulted in no lamination layer between the board and the aluminium layer. This made it possible to remove the aluminium- and inside layer from the rest of the packaging material. Material c (only inside layer) was produced by adding sheets of Mylar – PET films, before the second extruder. Due to poor adhesion between the Mylar sheet and the inside layer it was possible to peel off the inside layer without affecting it significantly. [3]

3.2 Tensile test

Specimens with dog bone shape were punched out from both material 1c and 2c and marked with paper dot markers in order for the extensometer to be able to track the extension. This can be seen in **Figure 3.1** a) and b).

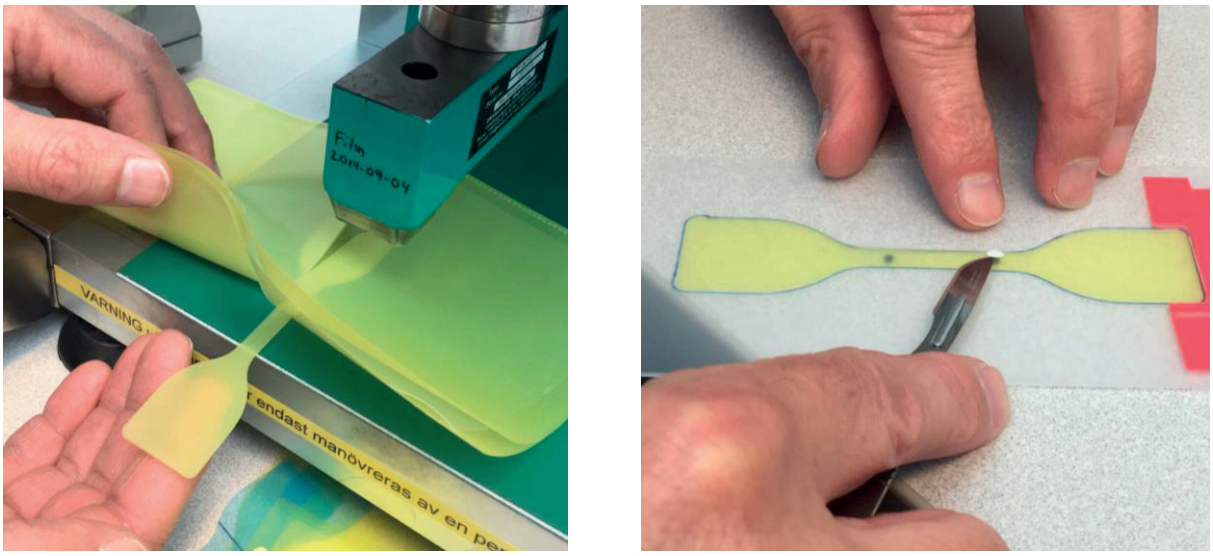

a ***b***

Figure 3.1 a) Dog bone shaped specimen for a tensile test **b)** Marking the specimen with paper dot markers

The narrow part of the dog bone was 6 mm wide and the spacing between the markers was 25 mm. The thickness of every sample was measured with a digimatic indicator from Mitutoyo. The samples were attached to the clamps in the tensile tester and pulled until break. A test in progress can be seen in **Figure 3.2**. Eight samples from each material were tested at speeds of 100, 150, 200 and 500 mm/min. The data points were plotted and analysed in Matlab.

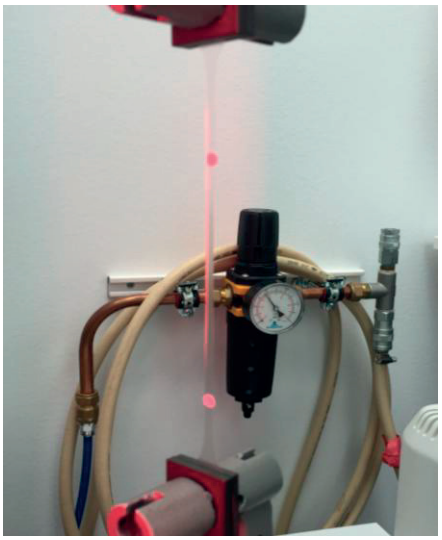

Figure 3.2 Picture of a tensile test in progress

4 Study 1

Study 1 consists of regular 90°- and 180° peel tests using ICPeel to obtain the adhesive fracture energy. The influence of elongation of the peel arm was considered. SEM was used to investigate board delamination and the thickness of the inside layer.

4.1 Method

To be able to compare the peel tests with different peel angles several equations were formed. An explanation for how the crosshead speed used in a test was calculated and how it corresponds to a certain crack propagation speed is followed by how peel tests are performed. The chapter continues with how to calculate which strain rate to use in a corresponding tensile test. The chapter ends with sections about ICPeel and how SEM was used.

4.1.1 Calculate the crosshead speed

Since the adhesive fracture energy is presumed to be rate dependant, it is of outmost importance that tests intended to be compared are performed at the same *crack propagation speed,* which is the speed with which the peel arm detaches from the rest of the sample. In order to obtain the same crack propagation speed for a 90° peel test and a 180° peel test, the difference in geometry must be taken into account. If the peel arm does not deform during the peel test, the relation between crosshead speed and crack propagation speed can be described as:

$$\dot{x} = \dot{a}(1 - \cos(\theta)) \tag{3}$$

Where $\dot{x}$ is the crosshead speed, $\dot{a}$ is the crack propagation speed and θ is the peel angle. This would result in a crosshead speed twice as high in the 180° case compared to the 90° case in order to obtain the same crack propagation speed.

However, the inside layer used as peel arm does indeed deform during a peel test. Since it deforms differently due to the different load cases in 90°- and 180° a term for this needs to be added to equation (3):

$$\dot{x} = \dot{a}(1 - \cos(\theta)) + \dot{\delta} \tag{4}$$

Where $\dot{\delta}$ is the elongation speed of the peel arm during a peel test.

4.1.2 How to obtain the same crack propagation speed

The plotted result for elongation speed vs. elongation speed can be seen in **Figure 4.5** a) and b) in section 4.2.1. From the difference in slope**,** a factor n can be calculated:

$$\frac{k_{90}}{k_{180}} = n \rightarrow \dot{\delta}_{90} = n\dot{\delta}_{180} \tag{5}$$

Where k is the slope in the elongation speed vs. crosshead speed curve. Using equation (4) the expressions for 90°- and 180° peel tests will be:

90° peel test: $$\dot{x}_{90} = \dot{a}_{90}(1 - \cos(90)) + \dot{\delta}_{90} \rightarrow \dot{x}_{90} = \dot{a}_{90} + \dot{\delta}_{90} \tag{6}$$

180° peel test: $$\dot{x}_{180} = \dot{a}_{180}(1 - \cos(180)) + \dot{\delta}_{180} \rightarrow \dot{x}_{180} = 2\dot{a}_{180} + \dot{\delta}_{180} \tag{7}$$

In order to be able to compare results for the adhesion values, the same crack propagation speed is required:

$$\dot{a}_{180} = \dot{a}_{90}$$

Combining this with equation (5), (6) and (7) gives:

$$\text{90° peel test:} \quad \dot{a}_{180} = \dot{x}_{90} - n\dot{\delta}_{180}$$

$$\text{180° peel test:} \quad \dot{a}_{180} = \frac{\dot{x}_{180}}{2} - \frac{\dot{\delta}_{180}}{2}$$

These two equations combined will result in:

$$\dot{x}_{90} = \frac{\dot{x}_{180}}{2} + \frac{\dot{\delta}_{180}}{2}(2n - 1) \tag{8}$$

Which can be used to calculate which crosshead speed should be used in the 90° peel test to obtain the same crack propagation speed as in the 180° peel test.

The crack propagation speed can be calculated by dividing the length of the crack obtained during the peel test with the propagation time. To estimate at what time the crack started to propagate, a bilinear fit can be fitted to the peel curve. During the first linear part the initial peel arm elongates until the crack starts to propagate and the peel force plateau is reached. At the plateau the crack propagation speed is assumed to be constant. A typical graph from a peel test with bilinear fit can be seen in **Figure 4.1**.

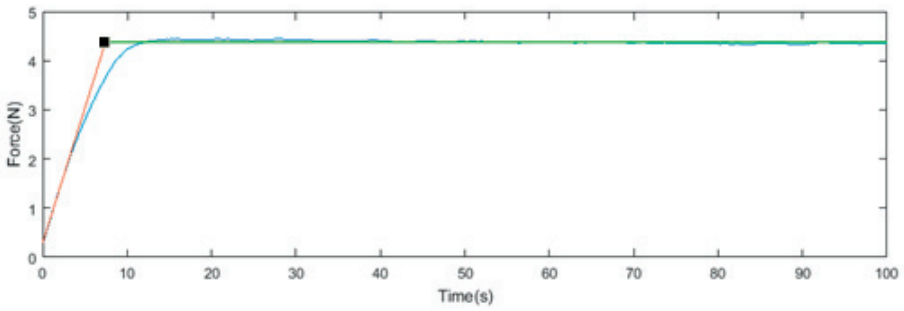

Figure 4.1 Typical graph from a peel test with a bilinear fit to extract the crack propagation speed

The crack length can be determined by marking the peel front before and after the peel test. The crack propagation speed can then be calculated:

$$\dot{a} = \frac{a}{t} \tag{9}$$

Where a is the crack length and t is the time it took for the crack to propagate the length a.

The elongation speed can then be calculated using equation (4):

$$\dot{\delta} = \dot{x} - \dot{a}(1 - \cos(\theta)) \tag{10}$$

4.1.3 Calculation of crosshead speed

The factor n and which crosshead speed to use in the 90° peel tests were calculated using equation (5) and (8):

Material 1a:

$$\frac{k_{90}}{k_{180}} = \frac{0{,}76}{0{,}54} = n_{1a} = 1{,}41$$

$$\dot{x}_{90} = \frac{\dot{x}_{180}}{2} + 0{,}91\dot{\delta}_{180} \tag{11}$$

Material 2a:

$$\frac{k_{90}}{k_{80}} = \frac{0{,}75}{0{,}49} = n_{2a} = 1{,}62$$

$$\dot{x}_{90} = \frac{\dot{x}_{180}}{2} + 1{,}03\dot{\delta}_{180} \tag{12}$$

The crosshead speed for the 180° peel test was chosen to 50 mm/min, and tests were performed on 10 specimens each for material 1a and 2a. The crack length was measured and the force-displacement curve from the peel test was fitted according to theory to extract the crack propagation time. An overview over the measurement results can be seen in appendix A.

The crack propagation speeds were calculated using equation (9). The elongation speeds were calculated using equation (10) with the average crack propagation speed. Thereafter, the crosshead speeds required in the 90° peel tests were calculated using equation (11) and (12) for material 1a and 2a respectively:

Material 1a:

$$\dot{\delta}_{180} = 50 - \dot{a}_{180}(1 - \cos(180)) = 25{,}10\ mm/min$$

$$\dot{x}_{90} = \frac{50}{2} + 0{,}91 \times 25{,}10 = 47{,}84\ mm/min$$

Material 2a:

$$\dot{\delta}_{180} = 50 - \dot{a}_{180}(1 - \cos(180)) = 24{,}35\ mm/min$$

$$\dot{x}_{90} = \frac{50}{2} + 1{,}03 \times 24{,}35 = 50{,}08\ mm/min$$

4.1.4 Sample preparation

The materials were produced on large rolls. To be able to test the materials smaller sample pieces had to be cut out. All samples were cut in the machine direction at the middle part of the roll using a guillotine. The samples had a width of 15 mm and a length of 50 mm. The width was measured more precise on every individual sample using a calliper. A part of the inside layer was peeled off from the aluminium layer by hand. The initial peeling induces a crack as well as creates a peel arm. Masking tape was applied 25 mm from the crack on the peel arm. This was done in order for the samples to have the same length of initial peel arm on all tests as well as reduce slip in the clamps. Before mounting the sample in the tensile tester the crack start was marked with a pen.

4.1.5 Peel tests

In a 180° peel test the sample was mounted in between the clamps in the tensile tester with the peel arm in a 180° angle in relation to the sample. When mounting a sample in the 90° test the lower clamp was switched out for a German wheel. Five tests were performed in both angles with crosshead speeds of 30, 40, 50, 60 and 70 mm/min with a displacement of 50 mm. Measurements with a crosshead speed of 50 mm/min in 180° and speed calculated on basis from theory in 90°, were performed with a displacement of 80 mm. When the test was complete the crack end was marked and the total crack length during the test was measured.

4.1.6 Strain rate in a peel test

The tensile properties of a material can be strain rate dependent. During a peel test the peel arm becomes longer both because of the propagation of the crack and the elongation of the peel arm. At the force plateau of the peel test the crack propagation speed is assumed to be constant, which means that the elongation speed of the peel arm must be constant as well. With a constant elongation speed and continuous addition of material, the strain rate of the peel arm changes during the course of the peel test.

If an assumption is made that all elongation of the peel arm occurs during a distance X from where the inside layer has detached from the substrate, the rest of the peel arm would be in a steady state with no elongation affecting it. This would isolate the strain to a small part of the peel arm close to the peel front. Furthermore, assuming that the strain is increasing linearly until becoming constant at the peel plateau (ε_p) would lead to the strain rate first being constant and becoming zero at the plateau region. A figure of strain vs. time and a schematic of the peel arm are presented in **Figure 4.2**.

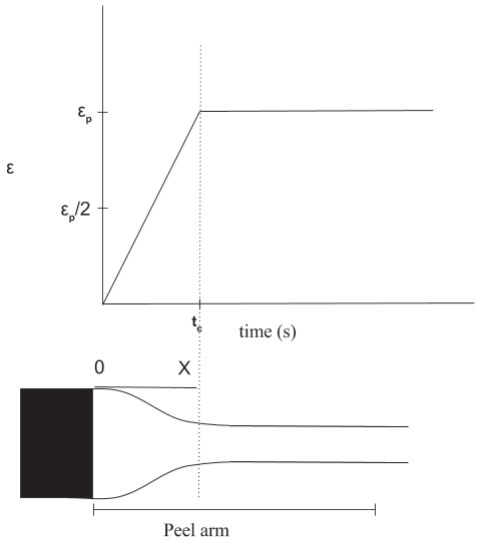

Figure 4.2 The figure on the top shows strain vs. time and the figure on the bottom shows how the length X is defined in the peel arm

The distance X consists of the elongation and crack length where:

$$X = a_x + \delta_x \tag{13}$$

Where X is the distance from the crack front to where the peel arm does not elongate anymore, a_x is the crack length and δ_x is the elongation of the peel arm.

The average strain at the linear region is $\frac{\varepsilon_p}{2}$, therefore:

$$\frac{\varepsilon_p}{2} = \frac{\delta_x}{a_x} \rightarrow \delta_x = \frac{a_x \varepsilon_p}{2} \tag{14}$$

Combining equation (13) and (14) gives:

$$X = a_x + \frac{a_x \varepsilon_p}{2} \rightarrow a_x = \frac{X}{\varepsilon_p + 2} \tag{15}$$

Since the crack propagation speed is constant at all times, the time it took to generate the crack a_x can be calculated by:

$$dt = \frac{a_x}{\dot{a}} \tag{16}$$

Where *dt* is the crack propagation time for a_x and $\dot{a}$ is the crack propagation speed. The strain rate is described by:

$$\dot{\varepsilon} = \frac{\varepsilon_p}{dt} \tag{17}$$

The strain rate during a peel test was calculated using equation (14-16) in combination with measurements of the length X. X was measured by taking pictures during the tests and measure the distance using the software ImageJ. Two parallel lines along the part of the peel arm with constant width (where the plateau is reached) were drawn, where the intersection of the lines and the peel arm edge marked where the elongation of the peel arm became constant. This can be seen in **Figure 4.3**.

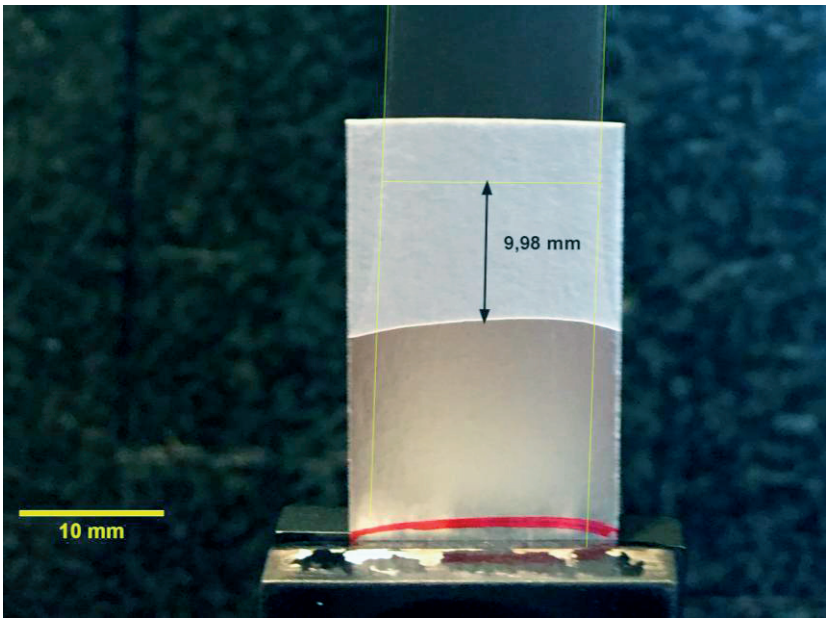

Figure 4.3 Picture of how the strain rate was determined. The black arrow denotes the distance X

4.1.7 ICPeel

The ICPeel method was applied by using a spreadsheet from Imperial College. [41] The spreadsheet has several input parameters, both material parameters and peel test parameters as well as the fit for the stress-strain curve. Both the bilinear fit and the power law fit were used separately. Among the output parameters were the total input energy and the adhesive fracture energy. The spreadsheet including results for both fits, both peel angles and both materials can be seen in appendix B.

4.1.8 SEM analysis

SEM was used for two analyses; to investigate if the board delaminated during peel tests and to investigate the thickness of the inside layer and whether the layer had any defects. To do this a cross section of the samples had to be prepared. This was done by fasten a piece of material between two Teflon plates. The Teflon plates and the material were cut in a cutting machine with a sharp knife. The thicknesses of the samples were 80 µm or 100 µm. To verify the quality of the cut they were analysed in a light microscope. The good quality samples were sputtered with gold particles before they were analysed in SEM. Both unpeeled and peeled samples were analysed. Samples that were very badly treated (folded and tugged by hand) in order to be assured that delamination in the board had occurred, were used as reference for how delamination appears in SEM images. The thickness of the inside layers were measured at a number of sites.

4.2 Result

4.2.1 Crosshead speed, crack propagation speed and elongation speed

The results from the investigation of how the crack propagation speed depends on the crosshead speed for 90°- and 180° peel tests for both material 1a and 2a can be seen in **Figure 4.4** a) and b).

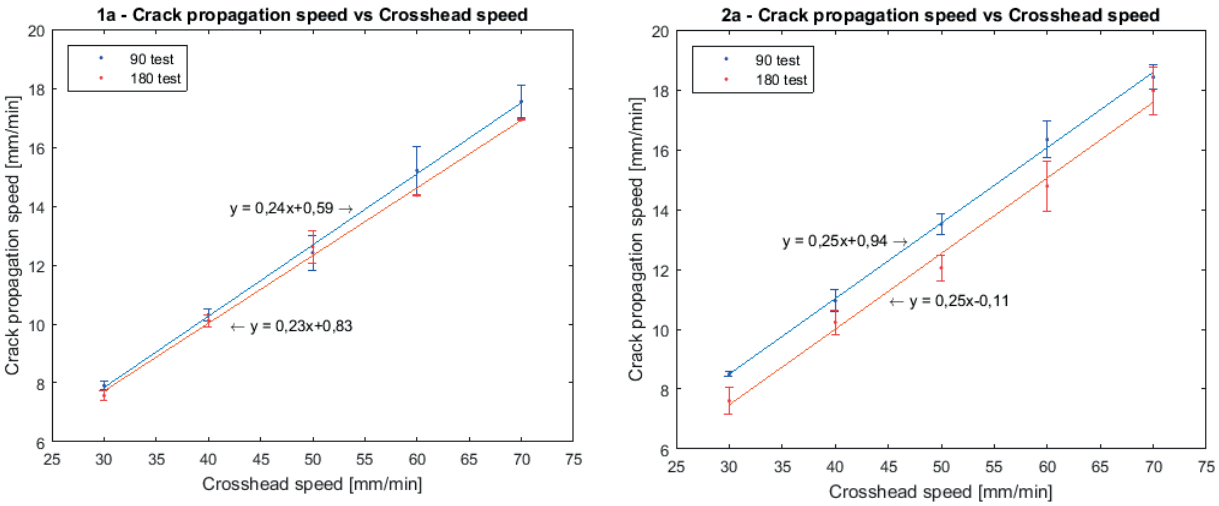

a **b**

Figure 4.4 Crack propagation speed vs. crosshead speed in 90° and 180° tests for **a)** material 1a **b)** material 2a

The results from the investigation of how the elongation speed depends on the crosshead speed for 90° and 180° peel tests for both material 1a and material 2a can be seen in **Figure 4.5** a) and b).

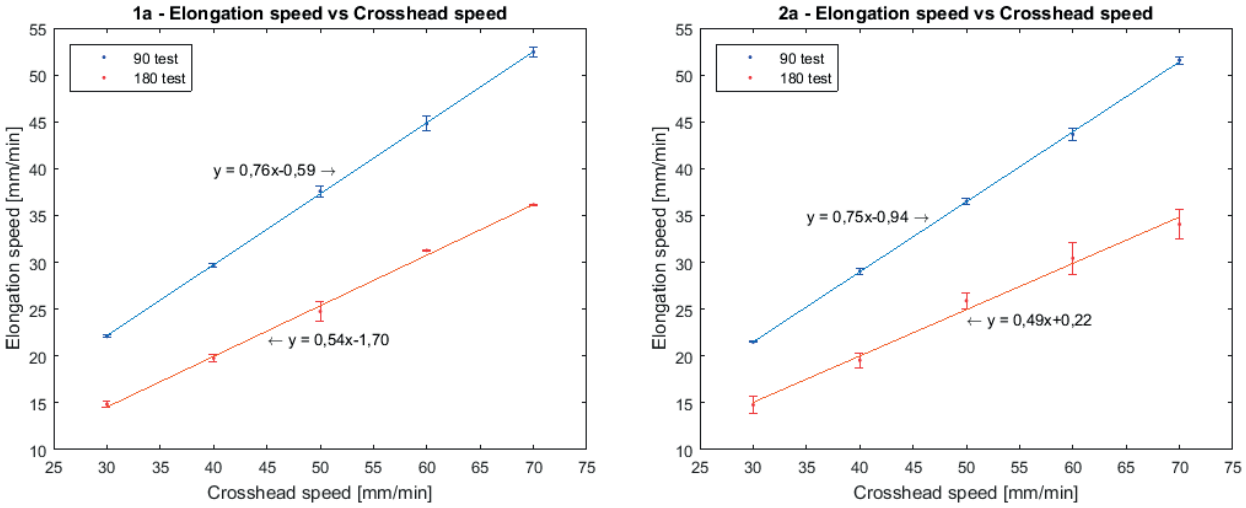

a **b**

Figure 4.5 Elongation speed vs. Crosshead speed in 90° and 180° tests for **a)** material 1a and **b)** material 2a

4.2.2 Tensile tests

The results of which crosshead speeds to use in the tensile tests for the materials are presented in **Table 2**.

Table 2 The different crosshead speeds which should be used in tensile tests for the different materials and peel angles

Material	Peel angle	Crosshead speed for tensile test (mm/min)
1a	90°	247
1a	180°	100
2a	90°	201
2a	180°	114

The thicknesses used in the calculations for the tensile test curves were a mean value from measurements made with the digimatic indicator; 54,7 µm for material 1 and 28,7 µm for material 2. The stress vs. strain curves for material 1c and 2c can be seen in **Figure 4.6** a) and b).

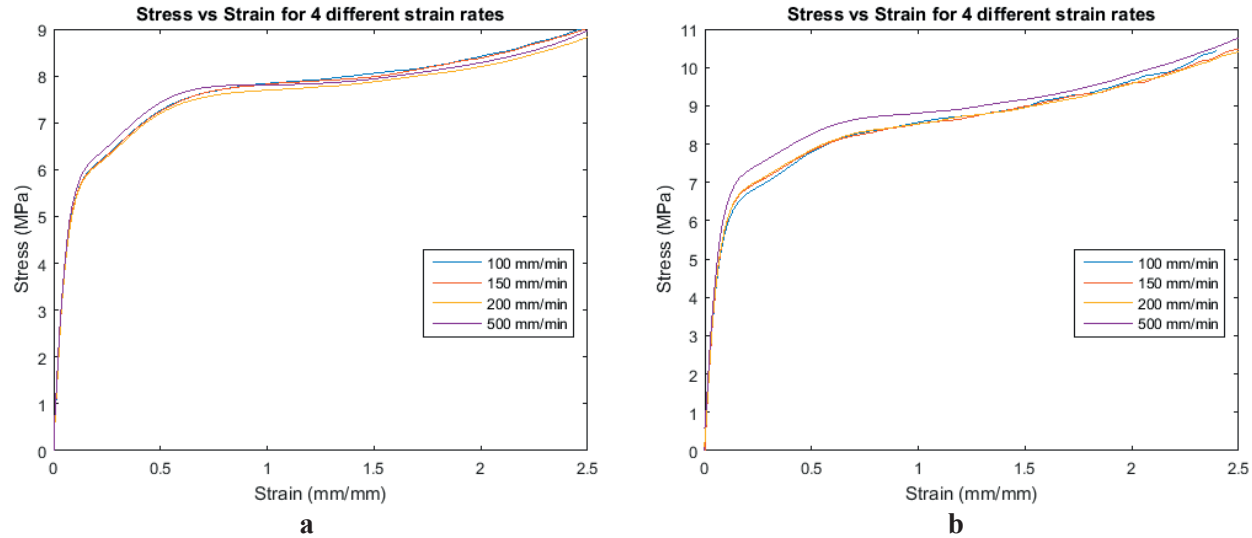

a **b**

Figure 4.6 Stress vs. strain curves with 4 different crosshead speeds for **a)** material 1c **b)** material 2c

4.2.3 ICPeel

An example of the two fits can be seen for the 100 mm/min stress-strain curve for material 1c in **Figure 4.7**.

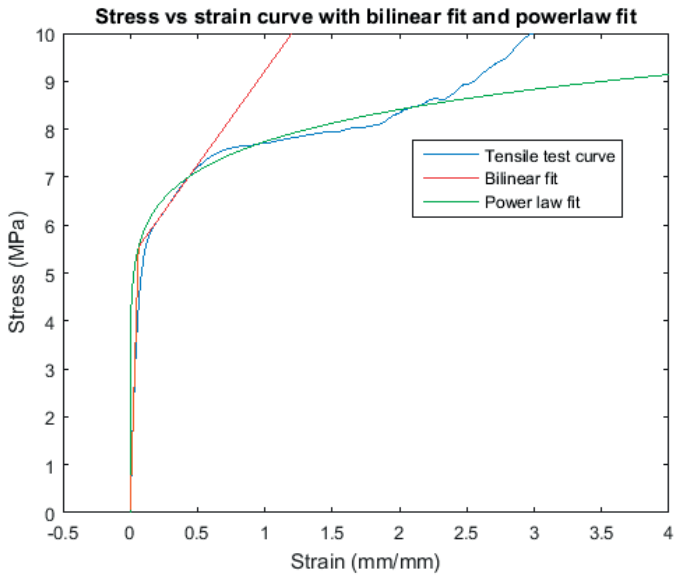

Figure 4.7 The two different fittings required in ICPeel for the 100mm/min tensile curve

The peel forces from the peel tests are plotted beside the results from ICPeel using the bilinear fit for both material 1a and 2a in **Figure 4.8** a) and b) respectively.

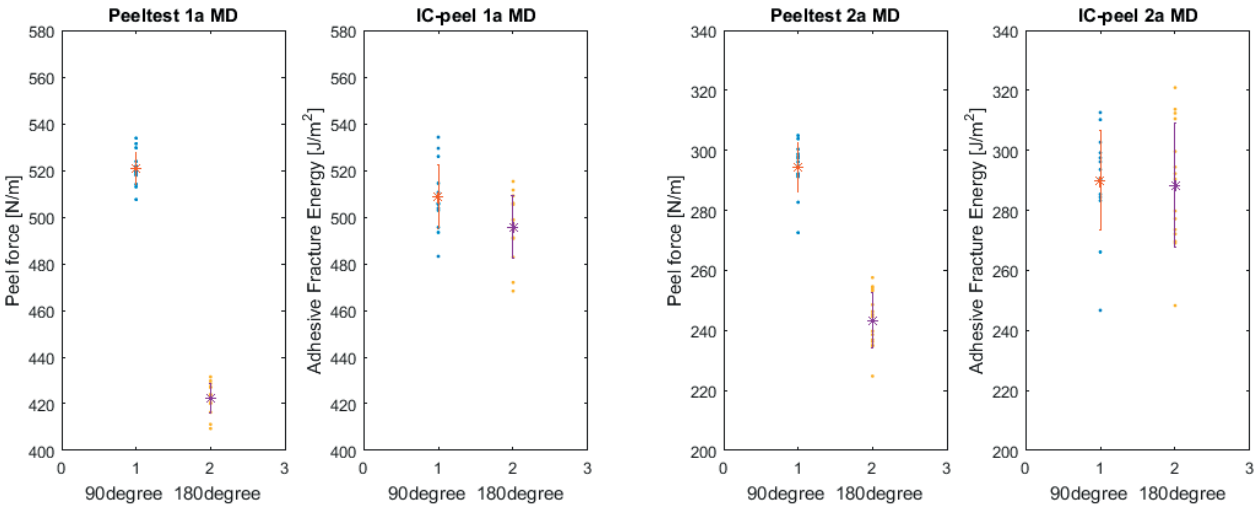

Figure 4.8 The results from peel tests and ICPeel using the bilinear fit for **a)** material 1a **b)** material 2a

The peel forces are plotted beside the results from ICPeel using the power law fit for both material 1a and 2a in **Figure 4.9** a) and b) respectively.

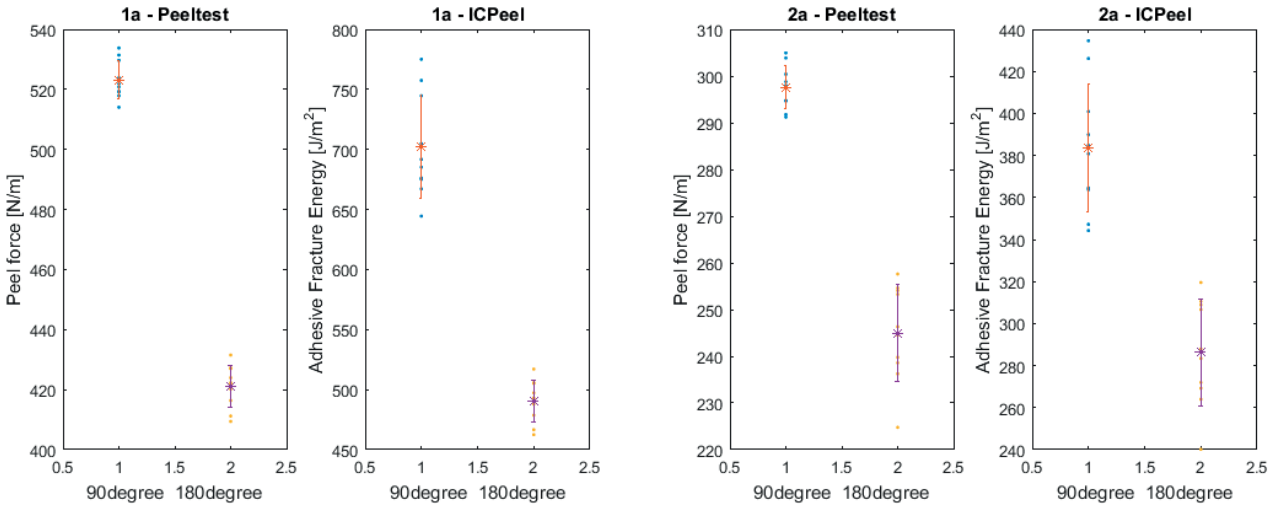

a **b**

Figure 4.9 The results from peel tests and ICPeel using the power law fit for **a)** material 1a **b)** material 2a

4.2.4 Board delamination

The SEM images of material 1a which has not been peeled and which has been peeled in 90° can be seen in **Figure 4.10** and **Figure 4.11**.

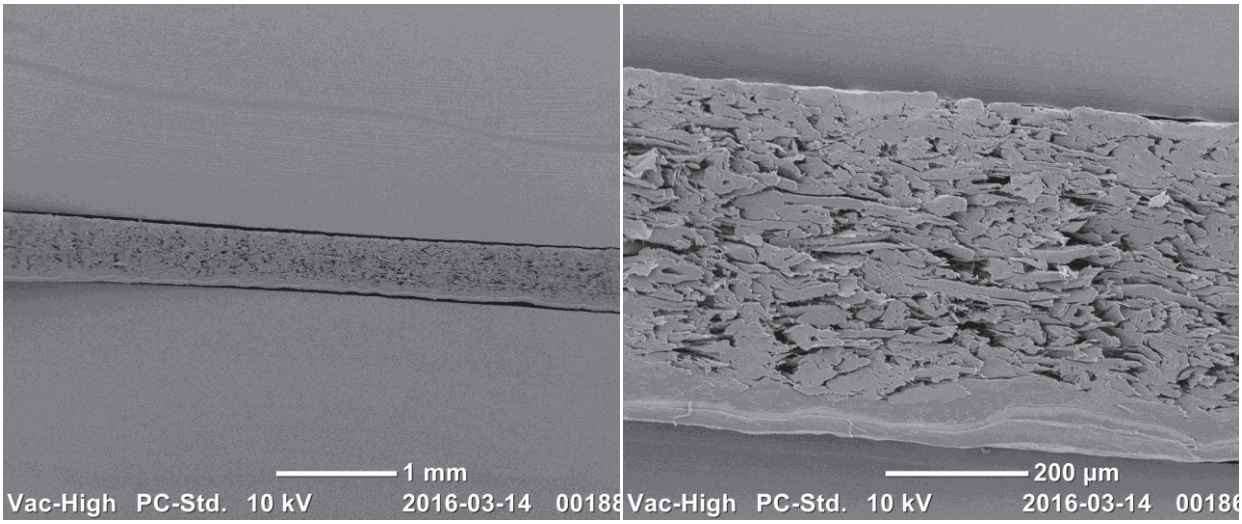

a ***b***

Figure 4.10 SEM images of unpeeled material 1a **a)** Magnification x220 **b)** Magnification x1300

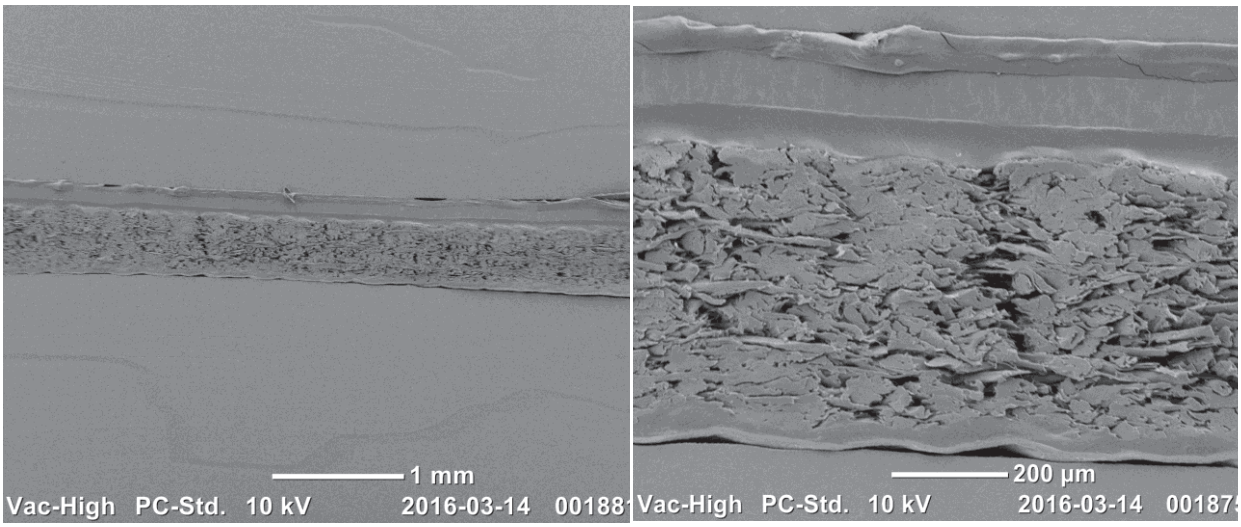

a ***b***

Figure 4.11 SEM images of material 1a which has been peeled in 90 ^{o} **a)** Magnification x220 **b)** Magnification x1100

The results from SEM- and light microscope images of badly treated material and untouched material can be seen in **Figure 4.12** and **Figure 4.13**.

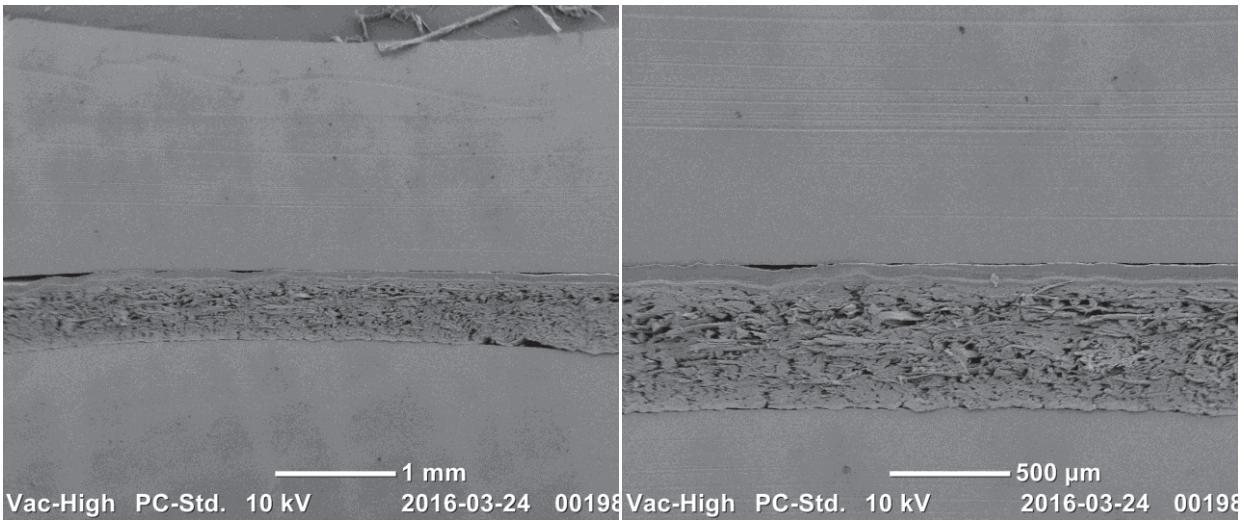

a ***b***

Figure 4.12 SEM images of material 1a which has been very badly treated **a)** Magnification x220 **b)** Magnification x440

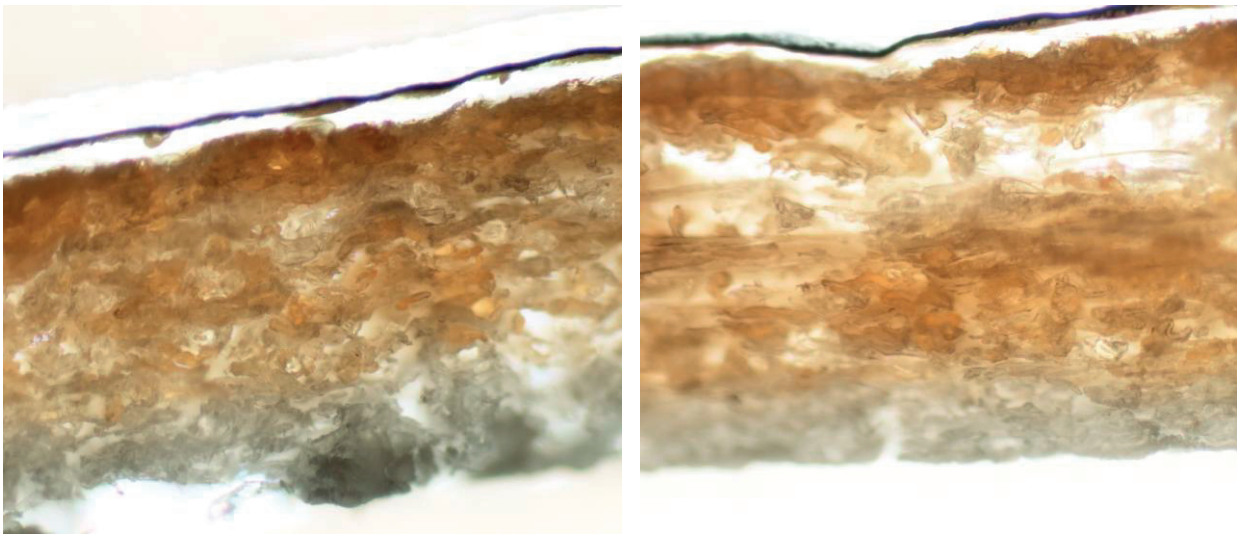

a *b*

Figure 4.13 Light microscope pictures of material 1a where **a)** is the untouched material **b)** is the badly treated material

4.2.5 Inside layer thickness

The SEM images from the measurement of the inside layer thickness can be seen in **Figure 4.14** a) and b).

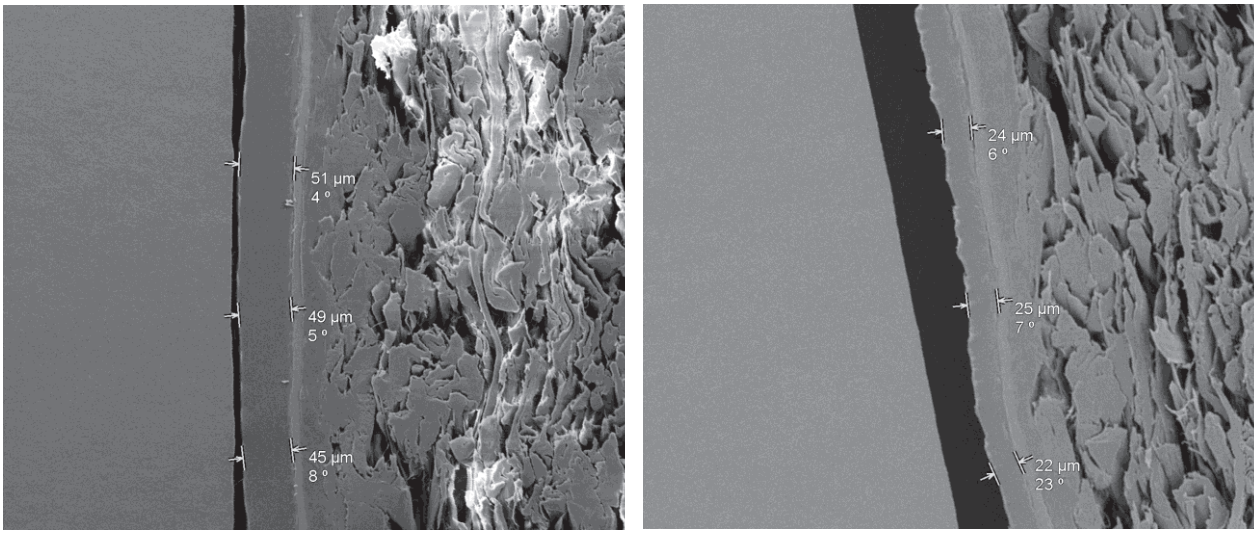

a *b*

Figure 4.14 SEM images with measurements of the inside layer thickness in **a)** material 1a magnification x2000 **b)** material 2a magnification x2000

For material 1 the thickness measured with the digimatic indicator varied from 52 µm to 59 µm with a mean value of 54,7 µm while the thickness measured in SEM varied from 44 µm to 58 µm. For material 2 the thickness measured with the digimatic indicator varied from 27 µm to 30 µm with a mean value of 28,7 µm while the thickness measured in SEM varied from 20 µm to 31 µm.

4.3 Discussion

4.3.1 Crosshead speed, crack propagation speed and elongation speed

The results in **Figure 4.4** show a linear correlation between crosshead speed and crack propagation speed, which were expected because of the direct connection between the speeds. The difference in load case for 90^{o}- and 180^{o} peel tests implies a difference in elongation, which is strengthened by the relationship between elongation speed and crosshead speed. This has to be considered when calculating which crack propagation speed a certain crosshead speed will result in.

A bilinear fit was used to isolate at what time the crack started to propagate. The adhesive fracture energy and the tensile properties of the peel arm are the critical factors for the force needed to separate the layers. Separation of the layers does not start until the force reaches a critical value, the force plateau. The crack propagation start point lies in the curved part of the peel curve where the force is converging to the plateau value. It was experimentally observed that the crack started to propagate in this region. Therefore the assumption of a bilinear behaviour in a peel test is reasonable.

4.3.2 Tensile test

The crosshead speed for the tensile test was estimated using several assumptions including that the strain during a peel test is increasing linearly until a plateau value where it becomes constant. If the strain were to be linearly increasing up to the plateau, the shape of the peel arm close to the peel front would too exhibit a linear tapering before sharply becoming constant in width. However, it was observed during the tests that the peel arm close to the peel front was having a curved shape. It would be preferred to calculate the actual mean strain considering the curved shape. The value of X in equation (13) was difficult to obtain with good precision due to difficulties with the focus in the pictures with the handheld cameras, the transparency of the peel arm and difficulty to determine where the tapered part of the peel arm ended. The margin of error in measuring the distance X leads to a bad correlation between the strain rate of the peel arm during peel test and its corresponding tensile test rate. The results from the tensile tests suggest that the materials used in this thesis were not strain rate dependant at the rates used. Therefore, the source of errors in estimating the strain rate could be neglected.

A more important aspect during the tensile tests was the influence of the inside layer thickness. A small modification of the thickness value was found to influence the results from the tensile tests to a great extent.

4.3.3 Inside layer thickness

The results from the SEM measurements of the inside layer thickness show varying thickness throughout the material for both material 1a and 2a. The variations were locally distributed, which leads to the digimatic indicator overestimating the thickness, since the relatively large stem is unable to reach the low points in the material.

In most applications the average thickness value is most relevant to use. However, when doing tensile measurements, the thinnest parts of the material will be subjected to the highest stresses leading to that this is where the rupture eventually will occur. Therefore, when measuring until break a value lower than the mean should be used. Since a successful peel test does not involve a break, the average thickness was used.

4.3.4 ICPeel

The ICPeel method was used with both bilinear and power law fits. ICPeel estimates the tensile energy in the peel test using the chosen fit and the peel force. Therefore, it is of importance that the fit represents the curve from the tensile test. For our material, the bilinear fit is only consistent with the tensile curve for very low strains whereas the power law fit seems reasonable to use with higher strains (see **Figure 4.7**). However, the estimated strains in the peel tests were out of range even for where the power law matched the tensile curve. The results from using the bilinear fit are in accordance with theory, in the sense of the adhesive fracture energy being the same for both peel angles, even though it was a poor fit for high strains in the tensile curve. The power law fit was a better fit to the tensile curve at higher strains while the results showed a big difference in adhesive fracture energy for the 90°- and 180° peel tests. The plots for ICPeel can be seen in **Figure 4.8** and **Figure 4.9**. This raised some concerns about the relevance of the ICPeel theory for our purposes. The inventor of the theory, Anthony Kinloch, was contacted and expressed doubt if his theory is valid for such large strains that occur when peel testing materials with as thin films as was used in this thesis.

If ICPeel is to be used for materials with large strains during peel tests, a correction in all terms would be required. A suggestion for treating the tensile deformation in the peel arm was made in the theory for 0° test. The more difficult term to express is the one addressing the local bending at the peel front. An alternative solution would be to only use ICPeel for materials with no or low strains in the peel arm during a peel test.

4.3.5 Board delamination

The SEM images of samples peeled in 90° compared to untouched material show no indication of board delamination, nor does the images of the very badly treated material. The fact that the badly treated material for sure had delaminated in the board but still did not exhibit this effect in the SEM images, indicates that this is not a suitable technique to examine if board delamination occurs. One reason why the delamination is not visible in SEM images could be that the board is pressed together between Teflon plates during the sample preparation. The light microscope pictures show a fracture in the board which could be interpreted as board delamination. However, it could also have been caused in the sample cutting process, therefore it is not suggested to use light microscope to investigate board delamination.

5 Study 2

A range of ideas for new methods to measure adhesive fracture energy were developed in study 2. The aim was to isolate or avoid complications with regular peel tests. Several ideas were based on using tape. The migration of the tapes used was investigated. All ideas were evaluated according to a number of criteria.

5.1 Ideas for alternative test setups

5.1.1 Peel test without board

Purpose: To investigate the influence of board delamination in peel tests.
The idea for this test method was to remove the board from the structure. To be able to compare results, tests in both 90° and 180° would be needed. The ideas for the test setups can be seen in **Figure 5.1** and **Figure 5.2**.

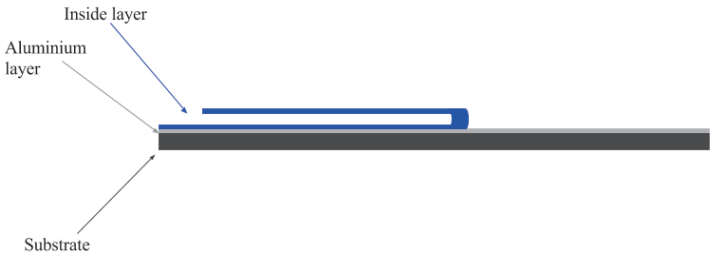

Figure 5.1 Test setup for 180° peel test without board

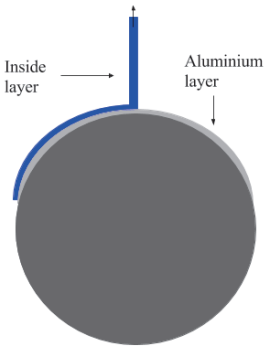

Figure 5.2 Test setup for 90° peel test without board

5.1.2 Reinforced inside as peel arm

Purpose: To avoid problems with thin peel arms.

Since problems in earlier peel test experiments could be due to that very thin peel arms are having properties which are not addressed in the ICPeel theory, a method that avoids the thin peel arms is desired. One way to do this is to reinforce the thin peel arm, and thus making it thicker. A crucial point in order for the method to work is to avoid delamination between the inside layer and the reinforcement material. This would be done by using a suitable adhesive. A schematic of the test material for a 180° test can be seen in **Figure 5.3**. A tensile test on the new peel arm consisting of the inside layer and the reinforcement needs to be made in order to use the ICPeel theory.

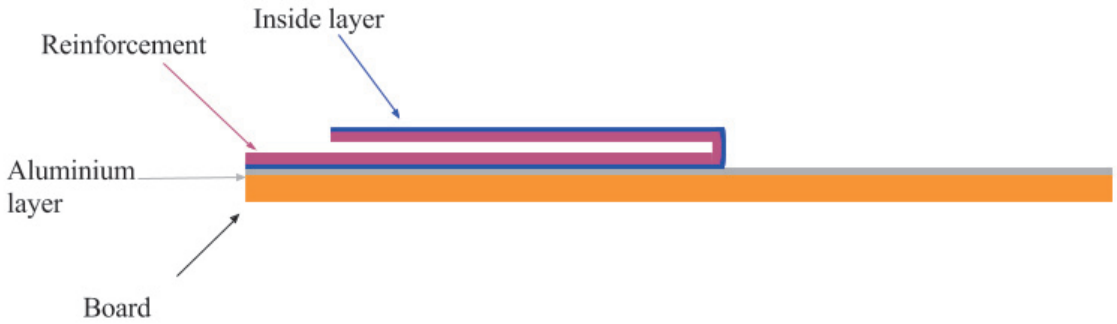

Figure 5.3 Test material for reinforced inside as peel arm

5.1.3 Reinforced aluminium as peel arm

Purpose: To avoid large deformations in thin peel arms.

Another approach to solve the thin peel arm problems is to use the aluminium layer as peel arm. Since aluminium layers in this thickness range (6-9µm) are too fragile in order to be used as peel arm by themselves, they would have to be reinforced. This could be done with either a thicker aluminium layer or with inside layer material (see **Figure 5.4**). One benefit of using the aluminium as peel arm is that most packaging materials have the same aluminium layer thickness, hence the test method would be more universal which would save a lot of work, for example not having to do as many tensile tests on the peel arms.

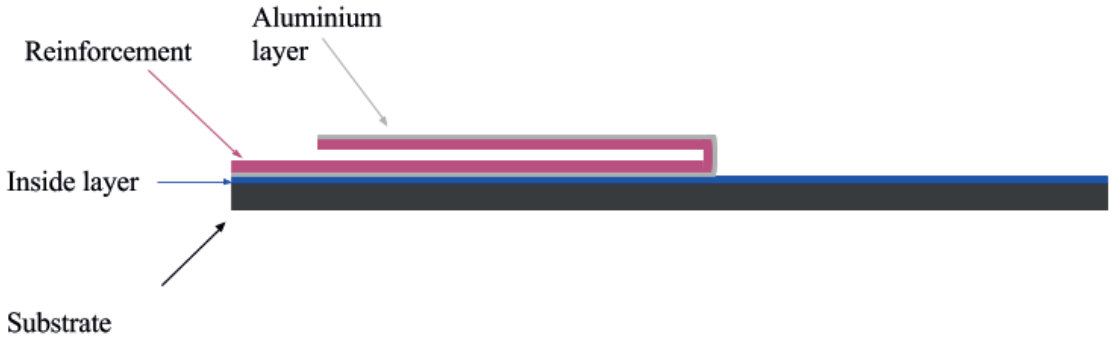

Figure 5.4 Test material for reinforced aluminium as peel arm

5.1.4 The DuckFace method

Purpose: To make a controllable z-direction test.

Designing a z-direction test is desirable since it would avoid earlier mentioned problems linked to the peel method, such as elongation, root rotation of the peel arm and the usage of ICPeel. However, a solution to the problems of being able to control between which layers the separation occurs is needed. To meet these requirements, the idea of the DuckFace method was developed. As can be seen in **Figure 5.5**, the DuckFace consists of two parallel and inflexible plates joined by a hinge. A specimen from material without board (material 1b/2b) is used to avoid energy losses due to board delamination. To direct the fracture into propagating between the desired layers, a small part of the specimen is peeled apart by hand. The sample is adhered to the DuckFace with the peeled parts adhered around the corners of the front part of the DuckFace (see **Figure 5.5**).

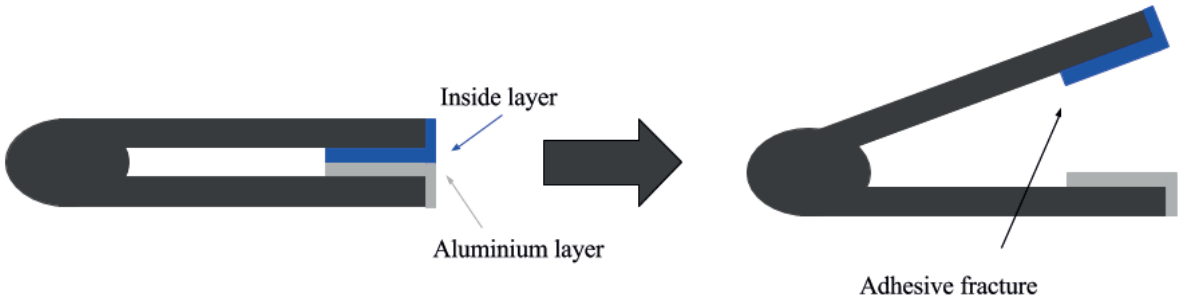

Figure 5.5 Test setup for the DuckFace method

5.1.5 One wheel method

Purpose: To avoid elongation of the peel arm.

The one wheel method aims to conduct a peel test with a set angle and no elongation of the peel arm by letting a wheel continuously support the peel arm. The sample is taped to a rigid substrate, part of the inside polymer layer is peeled off and taped on to the wheel (see **Figure 5.6**). When the wheel starts turning the peel arm is continuously adhered to the tape on the wheel surface.

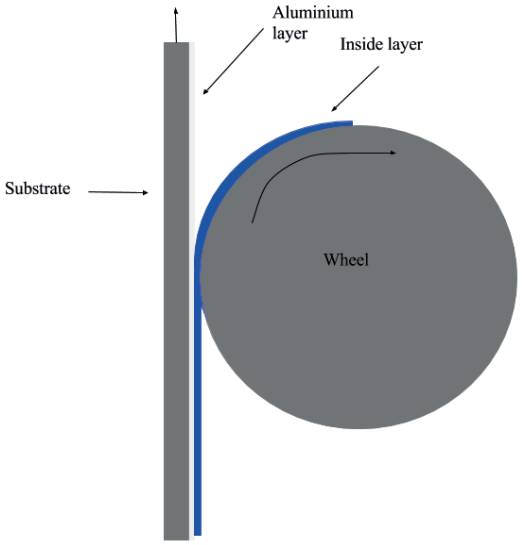

Figure 5.6 Test setup for the one wheel method

5.1.6 Two wheels method

Purpose: To avoid elongation of the peel arm.

The two wheel method aims to conduct a peel test with a set angle and no elongation of the peel arm. The aluminium layer and the inside layer are taped to one wheel each. The wheels are turned in opposite directions at the same rate and the peel arms are continuously taped to the wheels (see **Figure 5.7**).

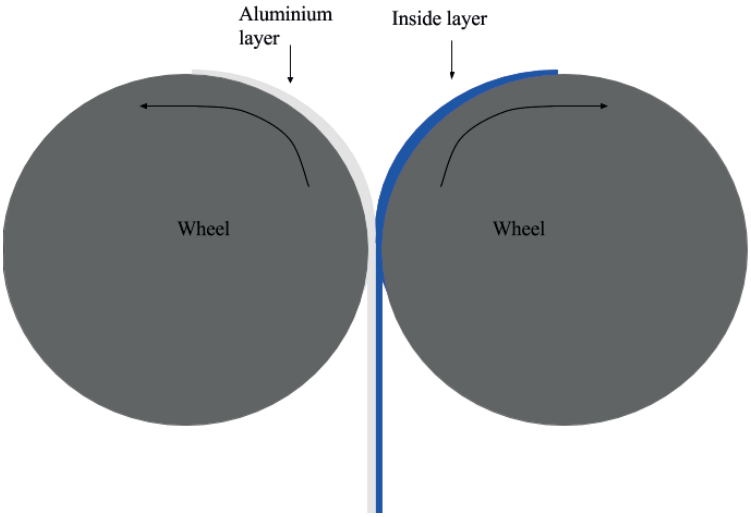

Figure 5.7 Test setup for the two wheels method

5.1.7 0° test

Purpose: To avoid bending of the peel arm.

Another idea of how to measure the adhesive fracture energy is to pull the peel arm in 0 degrees. This would introduce a load case for the system which measures the adhesive fracture energy in the x-y direction.

A 0° test would be performed by pulling a sample in an angle of 0° between peel arm and substrate. This would induce the peel arm to detach, not due to peeling as in a normal peel test manner but due to the elongation, and hence shrink in the dimensions orthogonal to the peeling direction, i.e. becoming thinner and narrower. A schematic sketch of this can be seen in **Figure 5.8**.

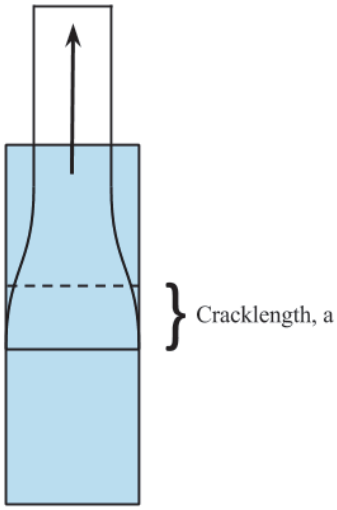

Figure 5.8 Schematic figure of a 0 ° test

5.2 Method

This chapter begins with an analysis of tape migration followed by an evaluation for the ideas for alternative test setups. Then the methods for five ideas chosen to proceed with are presented, including the formulation of an energy equation for the 0° test.

5.2.1 Tape migration analysis

Three tapes from 3M have been analysed, 5808 and 5809 which has no substrate and 9088 with a thin polyester substrate. FTIR measurements were conducted to investigate if the tapes migrated through the inside layer material. Since the inside consists of two layers (EAA and mPE) it is important on which side of the sample the analysis is done. EAA is facing the aluminium layer and is therefore the side which was examined. Pieces of tape were put on the mPE side and left for two days. Spectrum for the EAA side of the sample was obtained.

5.2.2 Evaluation of test methods

The author's ideas for test methods were evaluated according to a number of criteria, in order to determine which ones to proceed with. A summary of this can be seen in Table 3. Methods nr 1-4 and method nr 7 were chosen to proceed with, mainly due to time constraints and difficulties to obtain test setups consisting wheels.

Table 3 Criteria for test methods

	Problem avoided with method	Possible complications	Calculate adhesive fraction energy	Possible in time
1. Peel test without board	Delamination in board	Weak adhesion to substrate. Failure in aluminium	ICPeel	Yes
2. Reinforced inside as peel arm	Problems with thin peel arms	Weak adhesion to substrate or reinforcement. Failure in aluminium	ICPeel	Yes
3. Reinforced aluminium as peel arm	Elongation of peel arm. Differences between peel arms	Weak adhesion to substrate or reinforcement. Failure in aluminium	ICPeel	Yes
4. The DuckFace method	Uncontrolled crack propagation	Mixed mode failure. Adhesive too weak		Yes
5. One wheel method	Elongation of peel arm	Too weak continuous adhesion	ICPeel	No
6. Two wheels method	Elongation of peel arm	Too weak continuous adhesion	ICPeel	No
7. 0° test	Bending of peel arm	Not fully understood delamination mechanism	New energy equation	Yes

5.2.3 Peel test without board

Material b was taped onto a rigid substrate with the aluminium layer facing downwards. The samples were put under pressure for 1-3 days to optimise the adhesion to the tape. The inside layer was peeled off by hand from the aluminium layer.

5.2.4 Reinforced inside as peel arm

This method was conducted on material a. A crack was initiated by hand before the inside layer was reinforced by taping either a piece of material 1c or a piece of material 1b onto it. The samples were put under pressure for 1-3 days to optimise the adhesion to the tape. The reinforced inside layer was peeled off.

5.2.5 Reinforced aluminium as peel arm

Material 1b was used in this method. First a crack was initiated between the layers by hand whereafter the inside layer was taped to a rigid substrate. The aluminium was reinforced by taping either a piece of only inside material or a piece of material 1b onto it (see **Figure 5.9**). The samples were put under pressure for 1-3 days to optimise the adhesion to the tape. The reinforced aluminium peel arm was peeled off.

Figure 5.9 Samples with reinforced aluminium as peel arm

5.2.6 The DuckFace method

A prototype for the DuckFace model was created in Creo Parametric. The main purpose of this model was to get a brief overview over if the concept of the method works, hence the shaping details of the DuckFace were left to be further developed in a later prototype version. The model was printed in a 3D-printer and a provisional attachment for the tensile tester was made out of tape. Specimens from material 1b and 2b were cut into samples with different sizes and shapes, in order to evaluate which design is most promising. A crack between the aluminium layer and inside layer were initiated by hand. The specimen was then taped in the DuckFace and around its corners as can be seen in **Figure 5.10**. Rates from 10 to 50 mm/min were tested.

Figure 5.10 The DuckFace with taped sample mounted in the tensile tester

5.2.7 Energy equation for 0° test

A typical graph from a 0° test can be seen in **Figure 5.11** a). The energy needed to perform the test contains both the energy to detach the inside film from the aluminium layer and the energy needed to elongate the detached inside film. The energy needed to elongate the inside film can be calculated by using data from a true stress-strain diagram, which can be seen in **Figure 5.11** b).

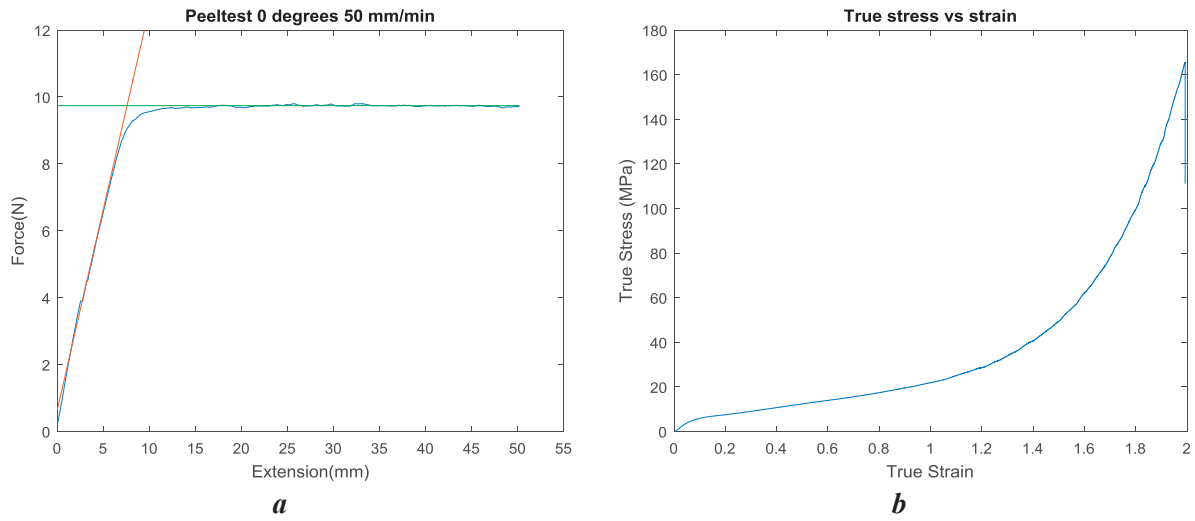

Figure 5.11 a) Plot from a typical 0° test **b)** Typical true stress-strain curve for the inside layer material

The energy during a 0° test can be expressed as:

$$G_{tot} = G_t + G_a \rightarrow$$

$$G_a = G_{tot} - G_t \tag{18}$$

Where G_{tot} is the total energy in the system during peel test plateau, G_t is the energy for tensile deformation of the peel arm during the peel test plateau and G_a is the adhesive fracture energy. In this model it is assumed that the only energy loss in the peel test is energy from tensile deformation of the peel arm.

The total input energy in the peel test, G_{tot}, can be expressed as:

$$G_{tot} = P * \delta \tag{19}$$

Where P is the force at the plateau during a 0° test and δ is the total elongation of the peel arm during the plateau. The total elongation can be calculated from the expression of true strain:

$$\varepsilon_t = l\,n\frac{\delta + a}{a} \rightarrow$$

$$\delta = a * (e^{\varepsilon_t} - 1) \tag{20}$$

Where ε_t is the true strain in the peel arm during plateau and a is the crack length. Combining equation (19) and (20) results in the equation:

$$G_{tot} = P * a * (e^{\varepsilon_t} - 1) \tag{21}$$

By assuming constant volume of the peel arm, the cross sectional area A of the peel arm at any strain, ε_t can be expressed as:

$$A = \frac{a * b * h}{\delta + a} = \frac{a * b * h}{a * ((e^{\varepsilon_t} - 1) + 1)} = \frac{b * h}{e^{\varepsilon_t}} \tag{22}$$

Where b is the specimen width at the start of the test and h is the specimen thickness at the start of the test. The expression for the energy lost due to elongation of the peel arm, G_t, can then be expressed by the integral from 0 to ε_t of the true stress-strain curve and the cross sectional area described in equation (22):

$$G_t = a * b * h \int_0^{\varepsilon_t} \frac{1}{e^{\varepsilon_t}} * \sigma_t(\varepsilon_t) d\varepsilon_t \tag{23}$$

Where $\sigma_t(\varepsilon_t)$ is the true stress. Combining equations (18), (21) and (23), and dividing by the area peeled off, $a * b$, the expression for the adhesive fraction energy can be written as:

$$G_a = \frac{P * a * (e^{\varepsilon_t} - 1) - a * b * h \int_0^{\varepsilon_t} \frac{1}{e^{\varepsilon_t}} * \sigma(\varepsilon_t) d\varepsilon_t}{a * b} \rightarrow$$

$$G_a = \frac{P * (e^{\varepsilon_t} - 1)}{b} - h \int_0^{\varepsilon_t} \frac{1}{e^{\varepsilon_t}} * \sigma(\varepsilon_t) d\varepsilon_t \tag{24}$$

5.2.8 0° test

The samples for the 0° test were cut out in dimensions 15 x 100 mm using a guillotine. Due to time constraints only material 1a was tested in 0°. The width was measured with a calliper and the inside layer thickness was measured with a LayerGauge from Davinor. A Davinor LayerGauge measures thickness by using the reflective index of the layers measured. [42] After the discovery of the overestimated thickness by the digimatic indicator the Davinor LayerGauge was used to measure the thickness with higher precision. This was discovered at a late stage of the thesis; therefore the Davinor LayerGauge was only used for the 0° tests. The inside layer was peeled off by hand from the aluminium layer to form a peel arm and to initiate a crack. The crack was marked and masking tape was applied 10 mm from the crack which can be seen in **Figure 5.12** a). The excess board was cut off to be able to mount the sample in the tensile tester. **Figure 5.12** b) shows a sample during a test. Two different studies were made in 0°; one with constant crosshead speed (50 mm/min) and varying displacement (75, 100, 125 and 150 mm) and one with a constant displacement of 100 mm and varying crosshead speed (25, 50, 100, 200 and 400 mm/min). The study with varying displacement length was made to confirm that the strain during the test is constant. The study with varying crosshead speed was conducted to investigate how the adhesive fracture energy in 0° tests is related to the crack propagation speed.

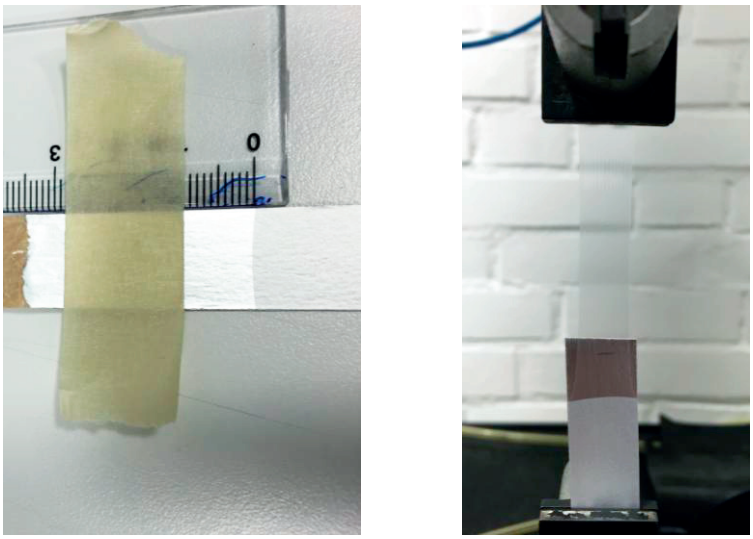

a **b**

Figure 5.12 Pictures from a 0° test **a)** Preparation of the sample where the peel arm is taped **b)** A 0° test in action

5.3 Result

5.3.1 Tape migration analysis

Material 1c and 2c with all three tapes were analysed. The spectra for the tapes are presented in **Figure 5.13**, the results from material 1c in **Figure 5.14** and material 2c in **Figure 5.15**. There are no big peaks between 2000 and 500 cm-1 which suggests that substances from the tapes do not migrate. Due to high similarity between the spectra of the materials and the spectrum for EAA (from a database), which was the material present on the surface, there is reason to conclude that no migration occurred.

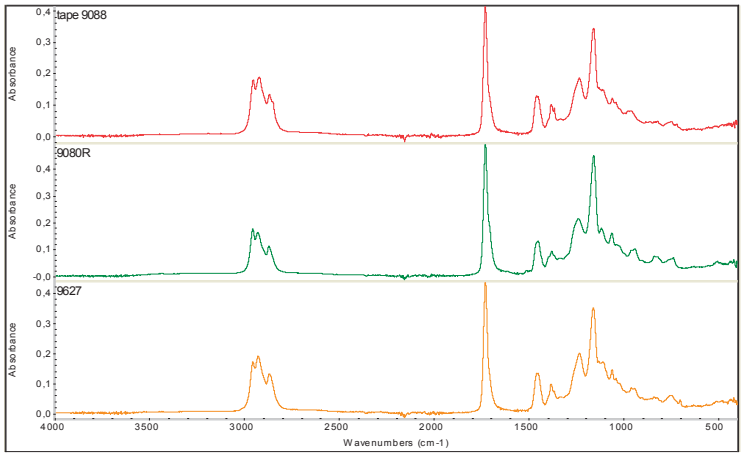

Figure 5.13 FTIR spectra for three tapes, from top to bottom: tape 9088, tape 9080R and tape 9627

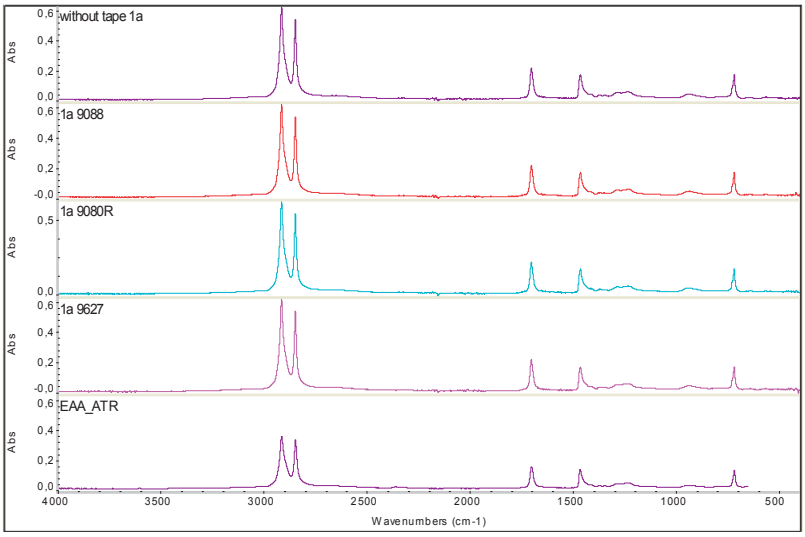

Figure 5.14 FTIR spectra for material 1c. From top to bottom: 1c without tape, 1c with tape 9088, 1c with tape 9080R, 1c with tape 9627, EAA (library match for the spectra)

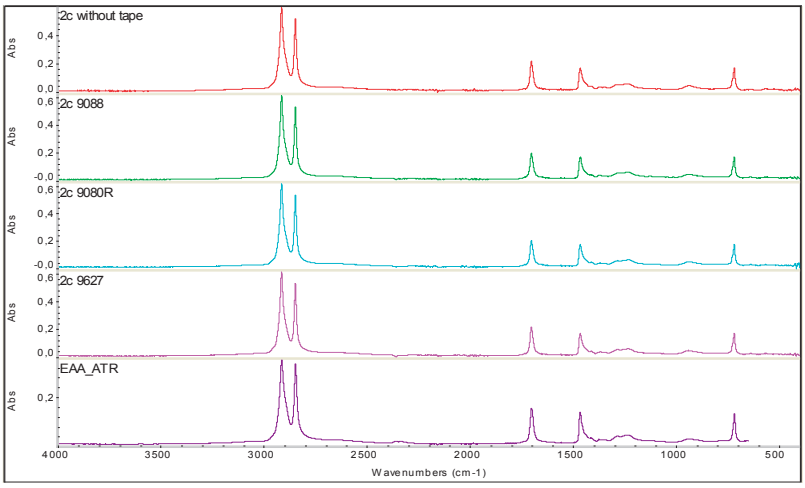

Figure 5.15 FTIR spectra for material 2c. From top to bottom: 2c without tape, 2c with tape 9088, 2c with tape 9080R, 2c with tape 9627, EAA (library match for the spectra)

5.3.2 Peel test without board

For this test material b was used. This material was believed to have defects due to irregularities and air bubbles that the full packaging material did not exhibit. During the peel tests, delamination between mPE and EAA occurred, which can be seen in **Figure 5.16**. Due to this it was not possible to obtain results corresponding to the adhesive fracture energy between the aluminium and inside layer.

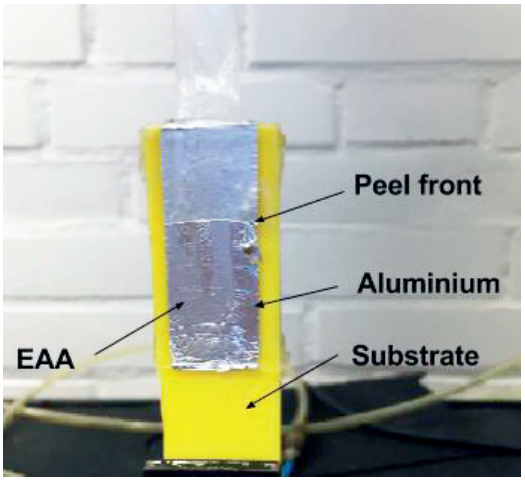

Figure 5.16 Failure between EAA and mPE and failure between the inside layer and the aluminium layer in a peel test without board

5.3.3 Reinforced inside as peel arm

None of the tapes had sufficient adhesion to reinforce the inside layer. The results from the 180^{o} peel test with this method were the same for all tests that were made, the reinforcement was peeled off from the inside layer at a higher rate than the inside was peeled off the aluminium (see **Figure 5.17**). The effect of this was two peel fronts instead of one. Hence no results of the adhesive fracture energy could be obtained.

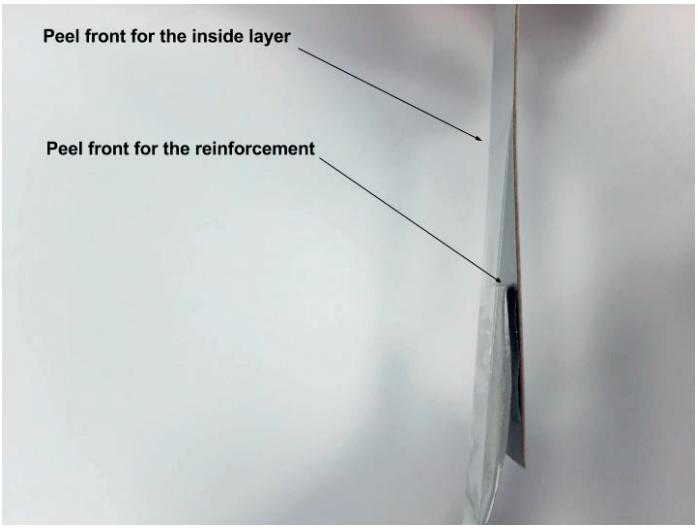

Figure 5.17 180° peel test with reinforced inside layer

5.3.4 Reinforced aluminium as peel arm

When the aluminium side was reinforced two problems in form of delamination in the wrong interface occurred; adhesive failure between the aluminium layers and adhesive failure between the substrate and the inside layer. In some cases the bottom aluminium layer cracked and caused delamination between the aluminium and the tape. These three cases are presented in **Figure 5.18** a), b) and c).

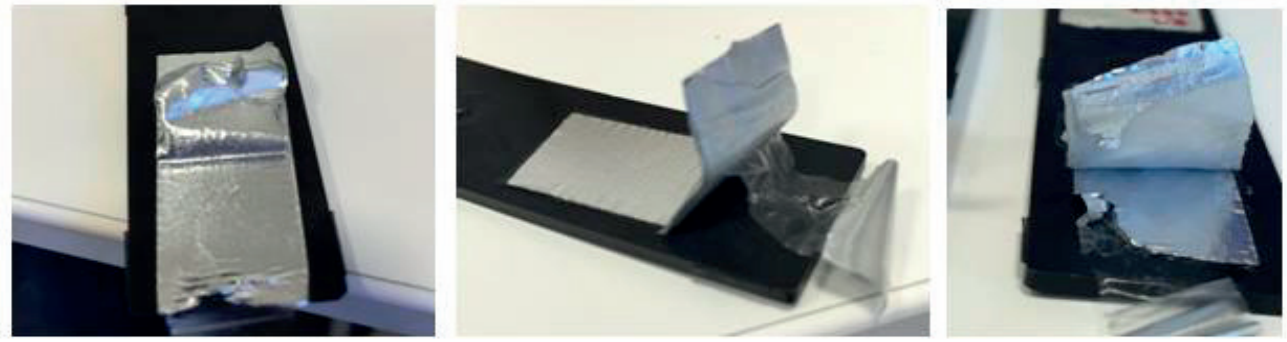

a **b** **c**

Figure 5.18 Failures when reinforcing the aluminium layer **a)** Adhesive failure between tape and aluminium layer **b)** Adhesive failure between substrate and the tape **c)** Cracked aluminium

5.3.5 The DuckFace method

Although the DuckFace method was tested with different specimen shapes and a variety of combinations of tapes and pulling rates, the attempts to obtain crack propagation between the aluminium layer and the inside layer failed. The high forces present, due to the high adhesion between the material layers, made the tape detach from the surface of the DuckFace on both sides of the specimen. In some cases separation between the tape and the inside layer could be seen. The DuckFace after a failed test can be seen in
Figure 5.19.

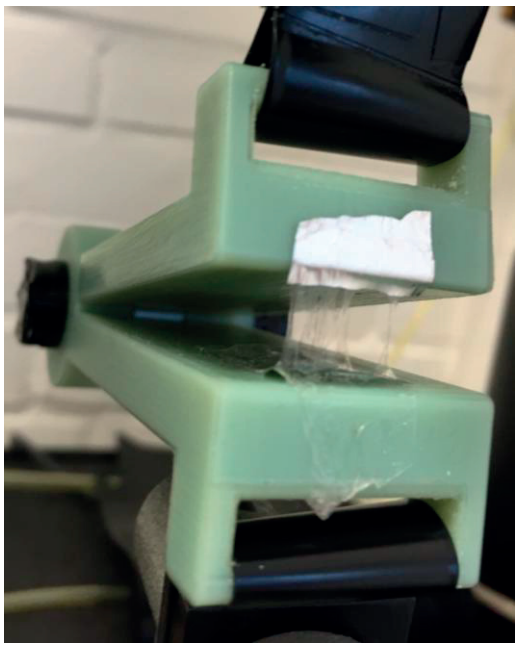

Figure 5.19 Failed DuckFace test

5.3.6 0° test

Matlab code used for the calculations of adhesive fracture energy for the 0° studies can be seen in appendix C.

5.3.6.1 Displacement study

The result from the displacement study can be seen in **Figure 5.20**.

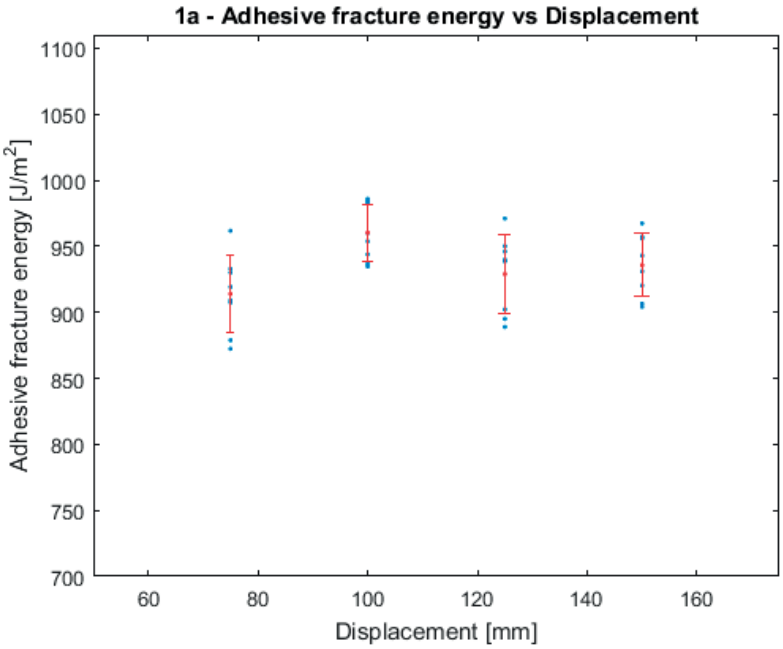

Figure 5.20 Adhesive fracture energy vs. displacement

The results from the displacement study indicate that the adhesive fracture energy does not depend on the displacement. Hence the same measurement data were used to investigate how the adhesive fracture energy was affected by the thickness of the sample. This is shown in **Figure 5.21** a) and b).

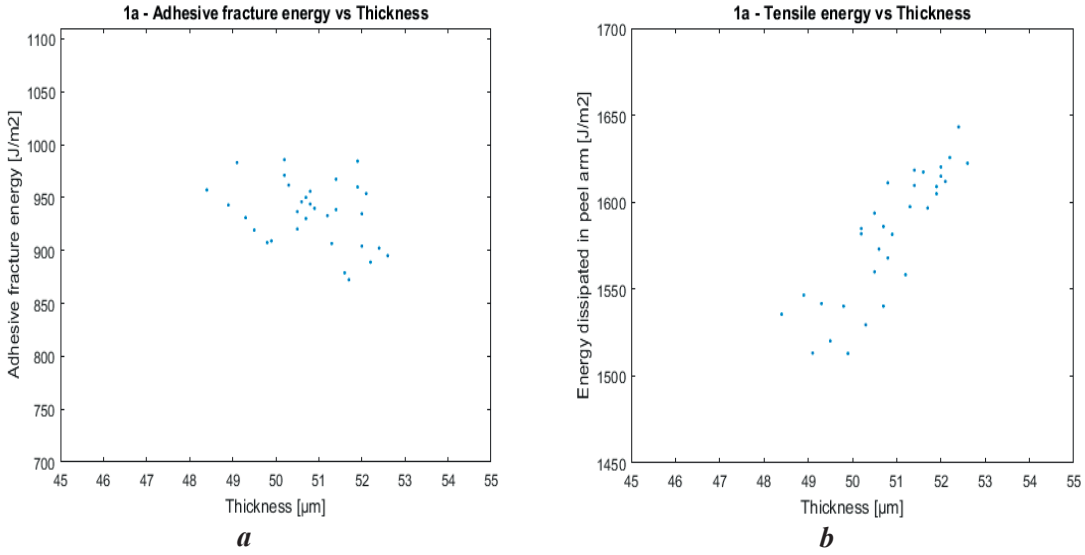

Figure 5.21 Energies plotted against the thickness of the samples **a)** Adhesive fracture energy vs. thickness **b)** Tensile energy in the peel arm vs. thickness

5.3.6.2 Rate dependency study

The crack propagation speed was plotted against the crosshead speed to investigate how they were related in a 0° test. This can be seen in **Figure 5.22**.

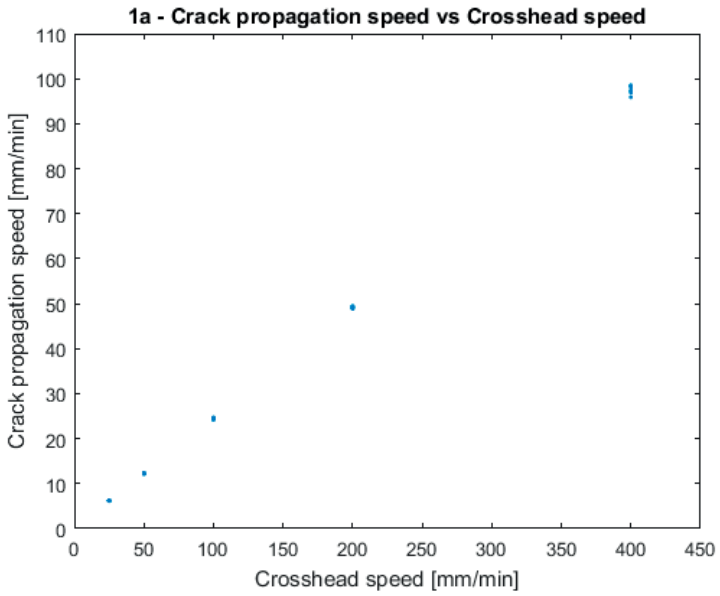

Figure 5.22 Crack propagation speed vs. crosshead speed for a 0^{o} test

The adhesive fracture energy for the 0^{o} tests was plotted against the crack propagation speed to investigate how the adhesive fracture energy changes with increasing crack propagation speed. This can be seen in **Figure 5.23**.

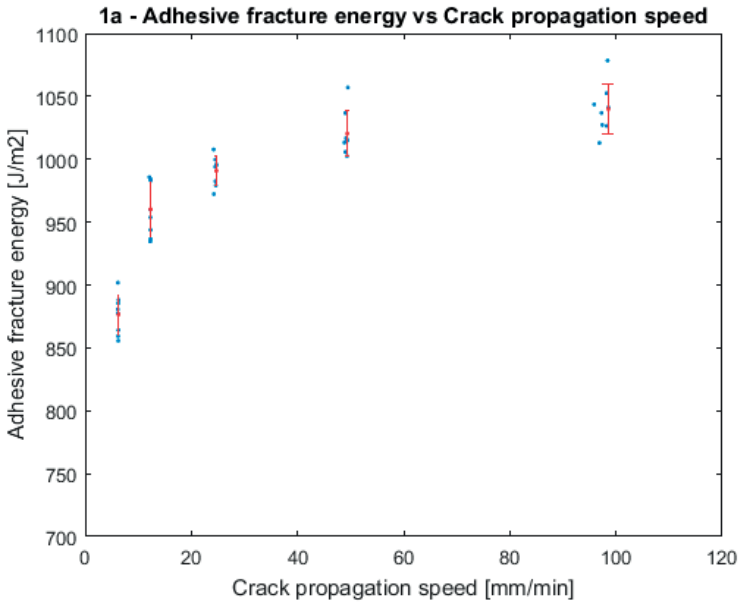

Figure 5.23 Adhesive fracture energy vs. crack propagation speed for a 0^{o} test

5.4 Discussion

5.4.1 Peel test without board

This method used material 1b and 2b in contrast to the other methods where material 1a and 2a were used. The results showed delamination in the inside layer between EAA and mPE, indicating that the characteristics of material b is not equivalent to the aluminium- and inside layer in material a. It has most likely either poorer adhesion between EAA and mPE or higher adhesion between EAA and the aluminium layer, causing the crack to propagate in another manner compared to in material a. It was visible for the naked eye that the surface of material b was not as smooth and even as in material a, but had some bubbles and irregularities. Thus, it is not applicable to compare results from tests on the material without board to the full packaging material.

5.4.2 Reinforced inside as peel arm

The tape did not adhere to the inside layer good enough in order for this method to work, the method is therefore difficult to evaluate. It should be noted that a tensile test on the peel arm is needed in order to determine material parameters which adds extra work and could be tricky for a reinforced peel arm.

5.4.3 Reinforced aluminium as peel arm

The same problems with the tape being too weak as in the method with reinforced inside as peel arm appeared in this method. Another drawback with the method is that material without board must be used (material 1b/2b) which both require additional work during the production process and verification that the material has the same characteristics as the full packaging material.

5.4.4 The DuckFace method

To be able to evaluate this method a strong adhesive is needed. The adhesive needs to adhere well to both the DuckFace and the inside layer. To make this easier the DuckFace should be made of a different material, to facilitate the attachment to the DuckFace. Since this was a first prototype there is a lot of room for improvements concerning the design of the DuckFace. If material without board can be produced with the right properties or if the board can be removed from the full packaging material without affecting the adhesion and a suitable adhesive is found this method is promising.

5.4.5 0° test

The mechanisms detaching the inside layer from the aluminium layer in a 0° test were not investigated in this thesis. Though, the authors suggest that the activation of the mechanisms is due to the elongation of the peel arm. If the peel arm do not elongate, either the whole inside layer would detach at the same time or the peel arm would break. The elongation induces shrinkage of the peel arm dimensions, which is believed to generate shear forces at the interface between the peel arm and the aluminium. This could be a cause for the detachment.

A limitation for the 0° test compared to a 90° peel test or especially a 180° peel test is that the peel force needed to perform the test is higher. This will induce a higher stress for a given material, increasing the risk of peel arm rupture during a test. A benefit with the 0° load case is the conformity with the load case in reality, for example when opening the cap of a package.

5.4.5.1 Displacement study

The results exhibit no change in the adhesive fracture energy with increasing displacement (see **Figure 5.20**) which is in line with the theory of the strain in the peel arm being constant during the peel curve plateau.

The inside layer thickness of the samples were plotted against tensile energy and adhesive fracture energy (see **Figure 5.21**). The tensile energy displays a clear trend of increasing with increasing thickness. This was expected since it requires a higher force to elongate a thicker material than a thinner. The adhesive fracture energy does not display any clear correlation with thickness. The scattering of the adhesive fracture energy values can therefore not be explained by variations of the inside layer thickness. An explanation could be defects in the aluminium layer affecting its ability to create adhesion to the adhesive polymer.

5.4.5.2 Rate dependency study

The results showed a linear dependence between crack propagation speed and crosshead speed. This was expected due to the fact that the peel arm elongation during the tensile tests indicated rate independence.

A polynomial relationship can be observed between the adhesive fracture energy and the crack propagation speed (see **Figure 5.23**). The adhesive fracture energy shows rate dependence by increasing at low crack propagation speeds followed by eventually converging. The rate dependency for lower speeds could be explained by that different mechanisms become activated at different crack propagation speeds. Another possible explanation is that the polymer chains at the interface have time to relax in tests performed at lower speeds, which give rise to a lower adhesive fracture energy. Since the adhesive fracture energy showed rate dependence only at low test speeds and the tensile test data used was obtained at higher speeds, it would be desirable to investigate how the material used shows strain rate dependence at lower speeds. The results from the 0° tests are strengthening the theory for the method, since they are consistent with the theory of the adhesive fracture energy being rate dependent.

6 Adhesion discussion

There are different views of what “true adhesion” really means. When it refers to the forces keeping two surfaces together, it is an entirely appropriate expression. The tricky part comes when trying to measure a value for true adhesion. Methods which are measuring adhesion by the means of separating surfaces are not measuring the true adhesion, but the *adhesive fracture energy*. The value obtained for the adhesive fracture energy will differ depending on the conditions of the test method, such as geometry and crack propagation speed.

7 Conclusion

There are several aspects to consider when performing peel tests in order to obtain the adhesive fracture energy. It is important to be aware of that the adhesive fracture energy for the interface is affected by crack propagation speed, material properties of the peel arm and peel angle. In order to compare tests it is important that they are performed at the same crack propagation speed. To obtain the same crack propagation speed for different geometries, the difference in elongation speed must be considered. Tensile tests performed to obtain material properties should be conducted at the same strain rate as the peel arm was subjected to during the peel test, especially if the material properties are strain rate dependant.

The ICPeel method is generally not suited for the large deformations occurring in thin peel arms of polyethylene during peel tests. The ICPeel theory requires the peel arm to be attached to a rigid

substrate. It proved to be difficult to investigate whether the board was rigid or if it delaminated during a peel test. The ICPeel method is not suitable to use for the packaging materials at Tetra Pak, unless a test setup, such as reinforcing the peel arm, that reduces the large deformations in the peel arm is developed.

It was not possible to fully evaluate the ideas for the reinforcement methods due to that none of the tapes had sufficient adhesion. If an adhesive is to be used on thin films, it is important to confirm that substances from the adhesive are not migrating through the material and affecting the adhesion. If the board could be removed from the rest of the packaging material, the DuckFace method seems promising, but needs improvement of the design and a suitable adhesive for both the DuckFace surface and the test material.

The 0° test was the best suited method for obtaining the adhesive fracture energy for materials with large deformations. The precision in measuring the dimensions of the peel arm is critical for the results, both for the tensile test and for the 0° energy equation. The adhesive fracture energy exhibited rate dependence at low crack propagation speeds and converged at higher speeds. A limitation with the 0° test is that the peel arm needs to elongate in order for the crack to propagate. The force needed to do this is relatively high compared to regular peel tests, which could lead to rupture in the peel arm.

A question that has been present during the entire thesis work is “Does true adhesion exist?”. Backed by the results the authors answer this by: -Yes it does, but it is impossible to measure by separating the surfaces. However, the adhesive fracture energy can be calculated; as long as we are aware of that the test conditions are affecting the results.

The most important findings on the subject ‘measuring adhesion’ are:

- ICPeel is not suitable to use when having high strains in the peel arm
- The adhesive fracture energy can be obtained and is best measured with the 0° test
- True adhesion cannot be measured by separating two surfaces; instead the adhesive fracture energy for that specific separation can be calculated

7.1 Proposals for future work

The authors believe that the best way of continuing the work of measuring the adhesive fracture energy is to proceed with 0° tests. Several suggestions for how to continue the investigation are listed below:

- To do a more in-depth study about the rate dependency of the material by performing 0° tests with low crack propagation speeds in small intervals combined with doing tensile tests corresponding to these speeds.
- To investigate at what crack propagation speed the adhesive fracture energy converges.
- To understand the mechanism behind the fracture in 0° tests and thereby verify the energy equation.
- To continue testing other materials and several different inside layer thicknesses to investigate the limits of the method.

If having materials not containing board, the DuckFace method is proposed to be used for obtaining the adhesive fracture energy. To use this method a suitable adhesive for both the DuckFace surface and the material surfaces would be needed. It is also proposed to optimise the design of the DuckFace.

8 Bibliography

[1] “Tetra Pak in figures,” Tetra Pak, 2015. [Online]. Available: http://www.tetrapak.com/about/facts-figures. [Accessed 23 May 2016].

[2] “Protects what´s good,” Tetra Pak, 2016. [Online]. Available: http://www.tetrapak.com/about/protects-whats-good. [Accessed 23 May 2016].

[3] N. Toft, Discussions, Senior Technology Specialist and Supervisor, Tetra Pak, 2016.

[4] “Tetra Pak Packaging material,” [Online]. Available: http://www.tetrapak.com/packaging/materials. [Accessed 19 May 2016].

[5] “Environmental product declaration; Liquid FC,” Billerud Korsnäs, 2014.

[6] “PlasticsEurope,” [Online]. Available: http://www.plasticseurope.org/information-centre/education-portal/resources-room/abc-of-plastics/the-abc-of-polyethylene.aspx. [Accessed 14 May 2016].

[7] J. Cowie and V. Arrighi, Polymers: Chemistry and physics of modern materials, Taylor and Francis group, 2007.

[8] N. Karak, Fundamentals Of Polymers: Raw Materials To Finish Products, PHI learning private limited, 2009, p. 135.

[9] G. Robertson, Food packaging principles and practice, Taylor and Francis group, 2006.

[10] M. Groover, Fundamentals of modern manufacturing; materials, processes and systems, John wiley and sons, 2010, pp. 169-170.

[11] A. Peacock, Handbook of polyethylene; Structures, properties and applications, Marcel Dekker inc., 2000.

[12] A. Barnetson, Plastic materials for packaging, Rapra technology limited, 1996.

[13] H. Archie and S. João, Metallocene catalyzed polymerization: industrial technology, Springer Netherlands, 1999.

[14] DSM, “Important aspects of extrusion coating”.

[15] R. Adams, Adhesive bonding; Science, technology and applications, CRC press, 2005.

[16] A. Kinloch, Adhesion and adhesives: science and technology, Chapman and Hall, 1987.

[17] J. Comyn, Adhesion science, The royal society of chemistry, 1997, pp. 114-118.

[18] E. Andreasson, Discussions, Technology specialist, Tetra Pak, 2016.

[19] C. Manjoy, “Rate-dependent fracture at adhesive interface,” *J. Phys. Chem. B,,* p. 6562–6566, 1999.

[20] J. Comyn, Adhesion science, The royal society of chemistry, 1997, pp. 5-18.

[21] D. Pocius and A. Dillard, The mechanics of adhesion, Elsevier Science, 2002, pp. 296-299.

[22] “AZO materials,” Zwick Roell, 2013. [Online]. Available: http://www.azom.com/article.aspx?ArticleID=6052. [Accessed 16 May 2016].

[23] W. Callister and D. Rethwisch, Fundamentals of materials science and engineering: an inegrated approach, John Wiley & Sons, 2012, p. 202.

[24] “Instron,” [Online]. Available: http://www.instron.se/sv-se/our-company/library/test-types/tensile-test. [Accessed 16 May 2016].

[25] “Tensile testing,” ASM international, 2004.

[26] S. Bernard, J. Roel, G. Leon and M. Han, “Intrinsic deformation behaviour of semicrystalline polymer,” 2003.

[27] Z. Bartczak and A. Galeski, “Plasticity of semicrystalline polymers,” *Macromol. Symp.,* pp. 67-90, 2010.

[28] J. Roesler, H. Harders and M. Baeker, Mechanical behaviour of engineering materials, Springer, 2006.

[29] H. Brinson and L. Brinson, Polymer engineering science and viscoelasticity an introduction, Springer, 2008.

[30] Instron, “Rotating German Wheel Peel Fixture, Catalog Number 2820-026,” Instron, 2005.

[31] A. Pizzi and K. Mittal, “Adhesion,” in *Handbook of adhesive technology*, Marcel Dekker, 1994, pp. 95-96.

[32] A. Kinloch, “The peeling of flexible laminates,” *International journal of fracture 66,* vol. 12, no. 42, 1994.

[33] L. Reimer, Scanning electron microscopy, physics of image formation and microanalysis, Springer, 1998.

[34] A guide to scanning microscope observation, JEOL, serving advanced technology, 2015.

[35] B. Norman, “Hur får man fibrer att lägga sig i en viss riktning?,” SkogsSverige, Institutionen för pappers- och massateknik, KTH, 2002.

[36] S. Norgren, P. Gradin, S. Nyström and M. Gullikson, “Investigation of Z-direction strength properties of paper by use of acoustic emission monitoring,” Mid Sweden University, 2008.

[37] B. Smith, Fundamentals of fourier transform infrared spectroscopy, CRC, 1996.

[38] T. N. Corporation, “Introduction to Fourier Transform Infrared Spectroscopy,” California Institute of Technology, 2001.

[39] F. Larsson, “Surface modification of LDPE using low temperature plasma for enabling adhesion measurements,” 2015.

[40] X. Lion and G. Geusken, “Adhesion of ethylene-acrylic acid copolymers and their blends with paraffin to aluminium,” *journal of adhesion science and technology,* vol. 13, pp. 669-678, 1999.

[41] A. Kinloch, C. Lau and J. Williams, “Imperial College London,” Imperial College, 2006. [Online]. Available: http://www.imperial.ac.uk/mechanical-engineering/research/mechanics-of-materials/polymers-adhesives-and-composites/adhesion/test-protocols/. [Accessed 2 May 2016].

[42] Davinor, [Online]. Available: http://www.davinor.com/content/en/1/90/LayerGauges.html. [Accessed 24 May 2016].

9 Appendix

Appendix A Results from peel tests

1a - MD 180° peel Displacement 80 mm. Sample 15*50 mm. Peel arm 25 mm long at t=0.							
Crosshead speed [mm/min]	**Sample nr**	**Force plateau [N]**	**Crack propagation start [s]**	**Crack length [mm]**	**Crack speed [mm/min]**	**Elongation speed [mm/min]**	**Width [mm]**
50	1	6,26	4,72	19,0	12,48	25,04	15,30
50	2	6,57	4,74	19,0	12,47	25,06	15,50
50	3	6,52	4,77	19,0	12,48	25,05	15,27
50	4	6,49	4,69	19,0	12,48	25,05	15,37
50	5	6,39	4,74	19,0	12,45	25,10	15,20
50	6	6,44	4,44	19,0	12,42	25,15	15,46
50	7	6,34	4,40	19,0	12,43	25,14	15,42
50	8	6,44	4,59	19,0	12,45	25,09	15,09
50	9	6,68	4,61	19,0	12,44	25,12	15,48
50	10	6,52	4,34	19,0	12,42	25,16	15,45

1a - MD 90° Displacement 80 mm. Sample 15*50 mm. Peel arm 25 mm long at t=0.							
Crosshead speed [mm/min]	**Sample nr**	**Force plateau [N]**	**Crack propagation start [s]**	**Crack length [mm]**	**Crack speed [mm/min]**	**Elongation speed [mm/min]**	**Width [mm]**
48	1	7,99	4,93	19,5	12,76	37,09	15,35
48	2	8,17	5,11	19,0	12,45	37,39	15,60
48	3	8,22	5,00	19,0	12,46	37,38	15,40
48	4	8,01	5,28	19,0	12,51	37,33	15,43
48	5	7,88	5,46	18,5	12,19	37,65	15,10
48	6	8,10	4,90	19,5	12,79	37,06	15,60
48	7	7,83	4,75	19,0	12,41	37,44	15,11
48	8	8,19	5,79	18,0	11,90	37,94	15,41
48	9	7,93	4,49	20,0	13,02	36,82	15,43
48	10	7,88	4,85	19,0	12,45	37,39	14,87

2a - MD 180° peel Displacement 80 mm. Sample 15*50 mm. Peel arm 25 mm long at t=0.							
Crosshead speed [mm/min]	**Sample nr**	**Force plateau [N]**	**Crack propagation start [s]**	**Crack length [mm]**	**Crack speed []**	**Elongation speed [mm/min]**	**Width [mm]**
50	1	3,78	4,73	19,0	12,50	25,04	15,46
50	2	3,51	5,07	21,0	13,80	22,36	15,61
50	3	3,70	4,77	20,0	13,10	23,71	15,02
50	4	3,63	4,78	20,5	13,50	23,05	15,20
50	5	3,59	4,28	21,0	13,70	22,61	15,20
50	6	3,85	4,17	19,0	12,40	25,25	15,17
50	7	3,93	3,84	19,0	12,30	25,35	15,27
50	8	3,83	4,01	19,0	12,40	25,27	15,14
50	9	3,87	4,11	18,0	11,70	26,55	15,19
50	10	3,62	4,19	19,0	12,40	25,20	15,11

2a - MD 90° Displacement 80 mm. Sample 15*50 mm. Peel arm 25 mm long at t=0.							
Crosshead speed [mm/min]	**Sample nr**	**Force plateau [N]**	**Crack propagation start [s]**	**Crack length [mm]**	**Crack speed [mm/min]**	**Elongation speed [mm/min]**	**Width [mm]**
50	1	4,32	4,21	20,8	13,33	35,78	14,85
50	2	4,48	4,02	21,0	13,42	35,69	14,70
50	3	4,37	4,35	22,2	14,26	34,85	14,99
50	4	4,43	4,67	21,0	13,52	35,59	14,84
50	5	4,48	4,34	21,0	13,47	35,64	15,05
50	6	4,55	4,40	20,9	13,39	35,72	15,26
50	7	4,49	4,12	20,1	12,85	36,26	15,23
50	8	4,34	4,57	20,8	13,38	35,73	14,74
50	9	4,69	4,42	19,9	12,75	36,36	15,44
50	10	4,58	3,98	19,9	12,71	36,40	15,23

Appendix B ICPeel spreadsheets

	Peel Arm Properties							Adhesive Layer		Test Parameters		Maximum (optional)	Results										
	E	σ_y (choose one)	ε_y	n (choose one)	α	h	b	h_a	E_a	P	θ	σ_{max}	G_C	G_d	G_{tot}	G	Correction	$\sigma_{max\ (0)}$	θ_0	k_0	R_a	ε_{max}	Loading / Unloading condition
	GPa	MPa	%	Power Law	Bilinear	mm	mm	mm	GPa	N	deg	MPa	J/m²	J/m²	J/m²	J/m²	%	MPa	deg		mm	%	
1	**1a MD**	**48**	**mm/min**																				
2	0,09	5,58			0,04	0,05	15,35			7,99	**90**		508,56	144,53	653,08	520,81	27,75	97,33	43,18	9,02	0,05	56,75	3
3	0,09	5,58			0,04	0,05	15,60			8,17	**90**		514,49	144,89	659,38	523,84	27,66	97,90	43,25	9,04	0,05	56,84	3
4	0,09	5,58			0,04	0,05	15,40			8,22	**90**		534,21	146,18	680,39	533,79	27,38	99,75	43,50	9,09	0,05	57,18	3
5	0,09	5,58			0,04	0,05	15,43			8,01	**90**		505,79	144,31	650,10	519,37	27,79	97,06	43,13	9,01	0,05	56,69	3
6	0,09	5,58			0,04	0,05	15,10			7,88	**90**		510,56	144,62	655,19	521,83	27,71	97,52	43,20	9,03	0,05	56,77	3
7	0,09	5,58			0,04	0,05	15,60			8,10	**90**		505,46	144,28	649,74	519,20	27,79	97,03	43,13	9,01	0,05	56,69	3
8	0,09	5,58			0,04	0,05	15,11			7,83	**90**		502,92	144,11	647,04	517,89	27,83	96,79	43,09	9,00	0,05	56,64	3
9	0,09	5,58			0,04	0,05	15,41			8,19	**90**		529,44	145,91	675,35	531,43	27,46	99,31	43,45	9,08	0,05	57,11	3
10	0,09	5,58			0,04	0,05	15,43			7,93	**90**		495,56	143,61	639,17	514,05	27,94	96,08	42,99	8,98	0,05	56,51	3
11	0,09	5,58			0,04	0,05	14,87			7,88	**90**		525,96	145,64	671,60	529,66	27,50	98,98	43,40	9,07	0,05	57,04	3
12																							
13	**1a MD**	**50**	**mm/min**																				
14	0,09	5,58			0,04	0,05	15,30			6,26	**180**		468,32	392,22	860,53	818,81	47,90	93,40	84,95	17,75	0,02	111,65	3
15	0,09	5,58			0,04	0,05	15,50			6,57	**180**		498,86	399,28	898,14	847,90	47,09	96,40	85,98	17,96	0,02	113,01	3
16	0,09	5,58			0,04	0,05	15,27			6,52	**180**		505,97	400,85	906,82	854,50	46,91	97,08	86,21	18,01	0,02	113,31	3
17	0,09	5,58			0,04	0,05	15,37			6,49	**180**		495,29	398,53	893,82	844,59	47,19	96,05	85,87	17,94	0,02	112,87	3
18	0,09	5,58			0,04	0,05	15,20			6,39	**180**		490,78	397,52	888,30	840,36	47,30	95,61	85,73	17,91	0,02	112,67	3
19	0,09	5,58			0,04	0,05	15,46			6,44	**180**		482,81	395,63	878,44	832,76	47,51	94,83	85,45	17,85	0,02	112,31	3
20	0,09	5,58			0,04	0,05	15,42			6,34	**180**		471,98	393,16	865,14	822,41	47,81	93,76	85,08	17,78	0,02	111,83	3
21	0,09	5,58			0,04	0,05	15,09			6,44	**180**		505,39	400,78	906,17	854,01	46,93	97,03	86,20	18,01	0,02	113,30	3
22	0,09	5,58			0,04	0,05	15,48			6,68	**180**		515,26	402,88	918,14	863,06	46,68	97,97	86,51	18,07	0,02	113,70	3
23	0,09	5,58			0,04	0,05	15,45			6,52	**180**		494,35	398,27	892,62	843,68	47,21	95,96	85,84	17,93	0,02	112,82	3
24																							
25	**2a MD**	**50**	**mm/min**																				
26	0,10	6,36			0,03	0,03	14,85			4,32	**90**		283,28	82,48	365,76	291,21	28,32	105,44	42,92	8,68	0,03	56,42	3
27	0,10	6,36			0,03	0,03	14,70			4,48	**90**		312,62	84,29	396,90	304,95	27,64	110,77	43,56	8,80	0,03	57,25	3
28	0,10	6,36			0,03	0,03	14,99			4,37	**90**		284,40	82,55	366,95	291,75	28,29	105,65	42,95	8,68	0,03	56,45	3
29	0,10	6,36			0,03	0,03	14,84			4,43	**90**		299,19	83,49	382,69	298,79	27,94	108,36	43,28	8,75	0,03	56,89	3
30	0,10	6,36			0,03	0,03	15,05			4,48	**90**		296,19	83,31	379,50	297,38	28,01	107,82	43,22	8,74	0,03	56,80	3
31	0,10	6,36			0,03	0,03	15,26			4,55	**90**		297,52	83,37	380,89	297,99	27,98	108,06	43,24	8,74	0,03	56,83	3
32	0,10	6,36			0,03	0,03	15,23			4,49	**90**		290,67	82,94	373,61	294,76	28,14	106,81	43,09	8,71	0,03	56,63	3
33	0,10	6,36			0,03	0,03	14,74			4,34	**90**		290,40	82,93	373,33	294,63	28,15	106,76	43,08	8,71	0,03	56,63	3
34	0,10	6,36			0,03	0,03	15,44			4,69	**90**		310,24	84,13	394,37	303,87	27,69	110,35	43,50	8,79	0,03	57,18	3
35	0,10	6,36			0,03	0,03	15,23			4,58	**90**		302,69	83,68	386,37	300,40	27,86	109,00	43,34	8,76	0,03	56,97	3
36																							
37	**2a MD**	**50**	**mm/min**																				
38	0,10	6,36			0,03	0,03	15,46			3,78	**180**		290,43	228,72	519,14	489,08	46,76	106,77	87,44	17,67	0,01	114,93	3
39	0,10	6,36			0,03	0,03	15,61			3,51	**180**		248,28	219,30	467,58	449,55	48,78	98,72	84,88	17,16	0,01	111,57	3
40	0,10	6,36			0,03	0,03	15,02			3,70	**180**		294,44	229,56	524,00	492,65	46,60	107,50	87,67	17,72	0,01	115,23	3
41	0,10	6,36			0,03	0,03	15,20			3,63	**180**		277,19	225,99	503,18	477,17	47,36	104,30	86,70	17,52	0,01	113,96	3
42	0,10	6,36			0,03	0,03	15,20			3,59	**180**		272,15	224,86	497,01	472,49	47,59	103,35	86,40	17,46	0,01	113,56	3
43	0,10	6,36			0,03	0,03	15,17			3,85	**180**		312,38	232,98	545,37	508,08	45,86	110,73	88,59	17,91	0,01	116,44	3
44	0,10	6,36			0,03	0,03	15,27			3,93	**180**		320,91	234,55	555,46	515,22	45,52	112,23	89,01	17,99	0,01	116,99	3
45	0,10	6,36			0,03	0,03	15,14			3,83	**180**		310,53	232,67	543,20	506,54	45,93	110,40	88,50	17,89	0,01	116,33	3
46	0,10	6,36			0,03	0,03	15,19			3,87	**180**		313,68	233,26	546,94	509,20	45,81	110,96	88,66	17,92	0,01	116,53	3
47	0,10	6,36			0,03	0,03	15,11			3,62	**180**		279,80	226,54	506,34	479,55	47,24	104,79	86,85	17,55	0,01	114,15	3

	Peel Arm Properties							Adhesive Layer		Test Parameters		Maximum (optional)	Results										
	E	σ_y (choose one)	ε_y	n (choose one)	α	h	b	h_a	E_a	P	θ	σ_{max}	G_C	G_d	G_{tot}	G	Correction	$\sigma_{max\ (0)}$	θ_0	k_0	R_a	ε_{max}	Loading / Unloading condition
	GPa	MPa	%	Power Law	Bilinear	mm	mm	mm	GPa	N	deg	MPa	J/m²	J/m²	J/m²	J/m²	%	MPa	deg		mm	%	
1	**1a MD**	**48**	**mm/min**																				
2	0,09	5,58		**0,12**		0,05	15,35			7,99	**90**		685,24	147,25	832,49	520,81	28,27	112,98	43,02	8,99	0,05	56,54	3
3	0,09	5,58		**0,12**		0,05	15,60			8,17	**90**		704,79	147,62	852,41	523,84	28,18	114,58	43,09	9,00	0,05	56,64	3
4	0,09	5,58		**0,12**		0,05	15,40			8,22	**90**		775,07	148,94	924,01	533,79	27,90	120,16	43,35	9,06	0,05	56,98	3
5	0,09	5,58		**0,12**		0,05	15,43			8,01	**90**		676,22	147,05	823,27	519,37	28,31	112,23	42,98	8,98	0,05	56,49	3
6	0,09	5,58		**0,12**		0,05	15,10			7,88	**90**		691,72	147,35	839,07	521,83	28,24	113,51	43,04	8,99	0,05	56,57	3
7	0,09	5,58		**0,12**		0,05	15,60			8,10	**90**		675,15	147,03	822,18	519,20	28,32	112,14	42,98	8,98	0,05	56,48	3
8	0,09	5,58		**0,12**		0,05	15,11			7,83	**90**		667,13	146,86	813,99	517,89	28,36	111,48	42,94	8,97	0,05	56,44	3
9	0,09	5,58		**0,12**		0,05	15,41			8,19	**90**		757,44	148,67	906,12	531,43	27,98	118,78	43,30	9,05	0,05	56,91	3
10	0,09	5,58		**0,12**		0,05	15,43			7,93	**90**		644,50	146,30	790,79	514,05	28,46	109,57	42,83	8,95	0,05	56,30	3
11	0,09	5,58		**0,12**		0,05	14,87			7,88	**90**		744,68	148,40	893,08	529,66	28,02	117,78	43,24	9,04	0,05	56,84	3
12																							
13	**1a MD**	**50**	**mm/min**																				
14	0,09	5,58		**0,12**		0,05	15,30			6,26	**180**		462,48	396,04	858,52	818,81	48,37	92,82	87,35	18,25	0,02	114,81	3
15	0,09	5,58		**0,12**		0,05	15,50			6,57	**180**		497,28	402,71	899,99	847,90	47,50	96,24	88,46	18,48	0,02	116,27	3
16	0,09	5,58		**0,12**		0,05	15,27			6,52	**180**		505,76	404,18	909,94	854,50	47,30	97,06	88,71	18,53	0,02	116,59	3
17	0,09	5,58		**0,12**		0,05	15,37			6,49	**180**		493,13	401,96	895,10	844,59	47,59	95,84	88,34	18,46	0,02	116,11	3
18	0,09	5,58		**0,12**		0,05	15,20			6,39	**180**		487,93	400,95	888,89	840,36	47,71	95,34	88,17	18,42	0,02	115,89	3
19	0,09	5,58		**0,12**		0,05	15,46			6,44	**180**		478,73	399,23	877,95	832,76	47,94	94,43	87,88	18,36	0,02	115,51	3
20	0,09	5,58		**0,12**		0,05	15,42			6,34	**180**		466,62	396,84	863,46	822,41	48,25	93,23	87,49	18,28	0,02	114,99	3
21	0,09	5,58		**0,12**		0,05	15,09			6,44	**180**		505,16	404,04	909,20	854,01	47,31	97,00	88,68	18,53	0,02	116,56	3
22	0,09	5,58		**0,12**		0,05	15,48			6,68	**180**		517,09	406,08	923,18	863,06	47,05	98,14	89,02	18,60	0,02	117,01	3
23	0,09	5,58		**0,12**		0,05	15,45			6,52	**180**		492,04	401,70	893,74	843,68	47,61	95,74	88,30	18,45	0,02	116,05	3
24																							
25	**2a MD**	**50**	**mm/min**																				
26	0,10	6,36		**0,11**		0,03	14,85			4,32	**90**		344,26	84,12	428,38	291,21	28,89	116,24	42,47	8,59	0,03	55,83	3
27	0,10	6,36		**0,11**		0,03	14,70			4,48	**90**		434,56	86,00	520,56	304,95	28,20	130,60	43,11	8,71	0,03	56,66	3
28	0,10	6,36		**0,11**		0,03	14,99			4,37	**90**		347,21	84,22	431,43	291,75	28,87	116,74	42,51	8,59	0,03	55,87	3
29	0,10	6,36		**0,11**		0,03	14,84			4,43	**90**		389,93	85,19	475,12	298,79	28,51	123,71	42,83	8,66	0,03	56,30	3
30	0,10	6,36		**0,11**		0,03	15,05			4,48	**90**		380,74	85,00	465,74	297,38	28,58	122,24	42,77	8,65	0,03	56,22	3
31	0,10	6,36		**0,11**		0,03	15,26			4,55	**90**		384,73	85,06	469,79	297,99	28,54	122,88	42,79	8,65	0,03	56,24	3
32	0,10	6,36		**0,11**		0,03	15,23			4,49	**90**		364,52	84,62	449,14	294,76	28,71	119,61	42,64	8,62	0,03	56,05	3
33	0,10	6,36		**0,11**		0,03	14,74			4,34	**90**		363,75	84,62	448,36	294,63	28,72	119,48	42,64	8,62	0,03	56,05	3
34	0,10	6,36		**0,11**		0,03	15,44			4,69	**90**		426,13	85,88	512,02	303,87	28,26	129,33	43,07	8,71	0,03	56,61	3
35	0,10	6,36		**0,11**		0,03	15,23			4,58	**90**		400,90	85,41	486,32	300,40	28,43	125,44	42,91	8,67	0,03	56,40	3
36																							
37	**2a MD**	**50**	**mm/min**																				
38	0,10	6,36		**0,11**		0,03	15,46			3,78	**180**		283,41	233,15	516,56	489,08	47,67	105,47	88,41	17,87	0,01	116,20	3
39	0,10	6,36		**0,11**		0,03	15,61			3,51	**180**		240,18	223,83	464,00	449,55	49,79	97,09	85,70	17,32	0,01	112,65	3
40	0,10	6,36		**0,11**		0,03	15,02			3,70	**180**		287,93	233,92	521,85	492,65	47,48	106,31	88,63	17,91	0,01	116,49	3
41	0,10	6,36		**0,11**		0,03	15,20			3,63	**180**		269,21	230,43	499,64	477,17	48,29	102,79	87,62	17,71	0,01	115,16	3
42	0,10	6,36		**0,11**		0,03	15,20			3,59	**180**		263,96	229,32	493,28	472,49	48,53	101,78	87,30	17,64	0,01	114,74	3
43	0,10	6,36		**0,11**		0,03	15,17			3,85	**180**		308,90	237,32	546,21	508,08	46,71	110,11	89,61	18,11	0,01	117,78	3
44	0,10	6,36		**0,11**		0,03	15,27			3,93	**180**		319,55	238,84	558,40	515,22	46,36	111,99	90,05	18,20	0,01	118,35	3
45	0,10	6,36		**0,11**		0,03	15,14			3,83	**180**		306,66	237,01	543,66	506,54	46,79	109,71	89,52	18,09	0,01	117,66	3
46	0,10	6,36		**0,11**		0,03	15,19			3,87	**180**		310,53	237,56	548,09	509,20	46,65	110,40	89,68	18,13	0,01	117,87	3
47	0,10	6,36		**0,11**		0,03	15,11			3,62	**180**		271,96	230,98	502,93	479,55	48,17	103,32	87,78	17,74	0,01	115,37	3

Appendix C Matlab code for 0° tests

```
%% calculation of total input energy, tensile energy and adhesive fracture
energy. Stress and Strain from tensile curve.
rawdata = xlsread('displacement'); %eller 'speed'
b = rawdata(:,15).*10^-3;%width
h = rawdata(:,13).*10^-6;%thickness
a_c = rawdata(:,7); %cracklength
elongation = rawdata(:,10); %elongation
epsilon_e = elongation./a_c; %calculated the true strain
epsilon_t=log(1+epsilon_e); %strain at end of test for each sample
peelforce = rawdata(:,3); %peelforce for each sample
% b = ones(length(a_c))*15*10^-3; %width of the sample (measure them later.
Gatrue = ones(size(epsilon_t)); %just making an equal vector
Gtott = ones(size(epsilon_t)); %just making an equal vector
for k = 1 : length(epsilon_t) % obtain the place in stress/strain curve for
the different strains
here = find(Strain >= epsilon_t(k));
stop = here(1);
tstress=Stress(11:stop); %take only stress values up to epsilon_t
tstrain=Strain(11:stop); %take only strain values up to epsilon_t
Gtot=(exp(epsilon_t(k))-1).*peelforce(k)/b(k); % total input energy
area = 1./(1+log(tstrain)); %the current area of sample(*bh) for
crossection area
integral = area.*tstress;%incorporate the decreasing cross section area
Gt = trapz(tstrain, integral);%approximated integrale over the stress
strain curve
Gatrue(k)= Gtot-Gt*h(k);%get the adhesive energy for the sample
Gtott(k) = Gtot;
end
%% write to excel
crossheadspeed = rawdata(:,1);
samplenumber = rawdata(:,2);
crackspeed = rawdata(:,8);
displacement = rawdata(:,16);
T =table(crossheadspeed, displacement, samplenumber,peelforce,crackspeed,
Gatrue, Gtott);
T(1:length(Gatrue),:);
filename = '1a md 0 degree adhesion displacement study new tensile
curve.xlsx';
writetable(T,filename,'Sheet',1,'Range','A2', 'WriteVariableNames',false)
labels ={'Crossheadspeed(mm/min)','displacement(mm)', 'Sample number',
'Force plateau(N)', 'Crack propagation rate(mm/min)', 'Adhesive fracture
energy(J/m2)', 'total input energy(J/m2)'};
xlswrite(filename,labels);
```